Sirtuin 1 and 2 inhibitors enhance the inhibitory effect of sorafenib in hepatocellular carcinoma cells

María Paula Ceballos, Antonella Angel, Carla Beatriz Delprato, Verónica Inés Livore, Anabela Cecilia Ferretti, Alvaro Lucci, Carla Gabriela Comanzo, María de Luján Alvarez, Ariel Darío Quiroga, Aldo Domingo Mottino, María Cristina Carrillo

PII: S0014-2999(20)30828-1

DOI: https://doi.org/10.1016/j.ejphar.2020.173736

Reference: EJP 173736

To appear in: *European Journal of Pharmacology*

Received Date: 24 June 2020

Revised Date: 2 November 2020

Accepted Date: 4 November 2020

Please cite this article as: Ceballos, M.P., Angel, A., Delprato, C.B., Livore, V.I., Ferretti, A.C., Lucci, A., Comanzo, C.G., de Luján Alvarez, M., Quiroga, A.D., Mottino, A.D., Carrillo, M.C., Sirtuin 1 and 2 inhibitors enhance the inhibitory effect of sorafenib in hepatocellular carcinoma cells, *European Journal of Pharmacology*, https://doi.org/10.1016/j.ejphar.2020.173736.

Author contributions

María Paula Ceballos: Conceptualization, Methodology, Validation, Formal analysis, Investigation, Resources, Data curation, Writing - original draft, review & editing, Visualization, Supervision, Project administration, Funding Acquisition

Antonella Angel: Formal analysis, Investigation, Data curation, Visualization

Carla Beatriz Delprato: Formal analysis, Investigation, Data curation, Visualization

Verónica Inés Livore: Investigation

Anabela Cecilia Ferretti: Conceptualization, Investigation, Resources

Alvaro Lucci: Investigation

Carla Gabriela Comanzo: Investigation

María de Luján Alvarez: Conceptualization, Resources

Ariel Darío Quiroga: Conceptualization, Resources, Writing - review & editing

Aldo Domingo Mottino: Conceptualization, Resources, Writing - review & editing, Supervision, Funding Acquisition

María Cristina Carrillo: Conceptualization, Resources, Writing - review & editing, Supervision, Funding Acquisition

Sirtuin 1 and 2 inhibitors enhance the inhibitory effect of sorafenib in hepatocellular carcinoma cells

María Paula Ceballos[a*], Antonella Angel[a;1], Carla Beatriz Delprato[a;1], Verónica Inés Livore[a], Anabela Cecilia Ferretti[b], Alvaro Lucci[a,b], Carla Gabriela Comanzo[a], María de Luján Alvarez[a,b], Ariel Darío Quiroga[a,b], Aldo Domingo Mottino[a;2], María Cristina Carrillo[a,b;2*]

[1,2]These authors contributed equally to this work.

María Paula Ceballos[a*]: ceballos@ifise-conicet.gov.ar
Antonella Angel[a;1]: antoanpal@hotmail.com
Carla Beatriz Delprato[a;1]: cbdelprato@gmail.com
Verónica Inés Livore[a]: livore@ifise-conicet.gov.ar
Anabela Cecilia Ferretti[b]: ferretti@ifise-conicet.gov.ar
Alvaro Lucci[a,b]: lucci@ifise-conicet.gov.ar
Carla Gabriela Comanzo[a]: comanzo@ifise-conicet.gov.ar
María de Luján Alvarez[a,b]: alvarez@ifise-conicet.gov.ar
Ariel Darío Quiroga[a,b]: quiroga@ifise-conicet.gov.ar
Aldo Domingo Mottino[a;2]: mottino@ifise-conicet.gov.ar
María Cristina Carrillo[a,b;2*]: carrillo@ifise-conicet.gov.ar

[a]Instituto de Fisiología Experimental (IFISE), Facultad de Ciencias Bioquímicas y Farmacéuticas, CONICET, UNR, Suipacha 570, 2000-Rosario, Argentina.

[b]Área Morfología, Facultad de Ciencias Bioquímicas y Farmacéuticas, UNR, Suipacha 570, 2000-Rosario, Argentina.

Corresponding authors:

*María Paula Ceballos, PhD, Instituto de Fisiología Experimental (IFISE), Facultad de Ciencias Bioquímicas y Farmacéuticas, CONICET, UNR, Suipacha 570, 2000-Rosario, Argentina. Tel: +54 341 4305799. Fax: +54 341 4399473. E-mail: ceballos@ifise-conicet.gov.ar

*María Cristina Carrillo, PhD, Instituto de Fisiología Experimental (IFISE), Área Morfología, Facultad de Ciencias Bioquímicas y Farmacéuticas, CONICET, UNR, Suipacha 570, 2000-Rosario, Argentina. Tel: +54 341 4305799. Fax: +54 341 4399473. E-mail: carrillo@ifise-conicet.gov.ar

Abstract

Multidrug resistance (MDR) counteracts the efficiency of sorafenib, an important first-line therapy for hepatocellular carcinoma (HCC). Sirtuins (SIRTs) 1 and 2 are associated with tumor progression and MDR. We treated 2D and 3D cultures (which mimic the features of *in vivo* tumors) from HCC cells with sorafenib alone or in the presence of SIRTs 1 and 2 inhibitors (cambinol or EX-527; combined treatments). Cultures subjected to combined treatments showed a greater fall in cellular viability, proliferation (PCNA, cyclin D1 and Ki-67 expression and cell cycle analysis), migration and invasion when compared with cultures treated only with sorafenib. Similarly, combined treatments produced more apoptosis (annexin V/PI, caspase-3/7 activity) than sorafenib alone. Since cell cycle dysregulation and apoptotic blockage are reported mechanisms of MDR, the modulation found in PCNA, cyclin D1, Ki-67 and caspase-3/7 proteins by cambinol and EX-527 are probably playing a role in enhancing the sensitivity of HCC cell lines to sorafenib. EX-527 reduced MRP3 and BCRP expression in sorafenib-treated HCC cells. Since ABC transporters contribute to MDR, MRP3 and BCRP could be also influencing in the response of HCC cells to sorafenib. Overall, 2D and 3D cultures behave similarly except that 3D cultures were less sensitive to treatments, reinforcing the clinical relevance of the current study. Findings presented in this manuscript support a potential application for SIRTs 1 and 2 inhibitors since we demonstrated that these compounds enhance the inhibitory effect of sorafenib upon treatment of hepatocellular carcinoma cells lines.

Keywords: hepatocellular carcinoma; sorafenib; sirtuins; HCC cell lines; EX-527; spheroids

1. Introduction

Sorafenib is one of the first-line treatments for hepatocellular carcinoma (HCC); however, it only prolongs median overall survival by nearly 3 months (Faivre et al., 2020). One of the main reasons underlying this feature is the multidrug resistance (MDR) (Chen et al., 2015). MDR is a major cause of HCC recurrence and metastasis (Ceballos et al., 2019), with different resistance mechanisms against the same drug acting in the same tumor cell (Kartal-Yandim et al., 2016). Additionally, many patients require dose reduction to minimize adverse effects exerted by sorafenib (Gadaleta-Caldarola et al., 2015).

Sirtuins (SIRTs) are class III histone deacetylase enzymes. Among SIRTs members, SIRTs 1 and 2 are reported to play crucial roles in cellular proliferation, migration and invasion and in the blockage of apoptosis and are related to the promotion of tumor initiation, progression and metastasis in HCC (Chen et al., 2013; Li et al., 2016; Wu et al., 2015; Xie et al., 2011). These studies also showed a positive correlation between SIRTs 1 and 2 expression and poor prognosis in patients with this malignancy. SIRTs 1 and 2 are upregulated in HCC cell lines and in a subset of human HCC tissues when compared to normal hepatocytes and nontumoral tissues, respectively (Chen et al., 2013; Li et al., 2016; Portmann et al., 2013; Xie et al., 2011). Deacetylation of key cell cycle molecules and apoptosis regulatory proteins by SIRTs 1 and 2, including p53 and FoxO, abolishes the capability of these tumor suppressors to induce cell growth arrest and apoptosis (Wang et al., 2019). In this regard, dysregulation of cell cycle checkpoints and blockage of apoptotic signals are mechanisms involved in MDR (Kartal-Yandim et al., 2016). At the same time, it was demonstrated that SIRT1 overexpression in HCC cells induces the upregulation of P-glycoprotein (P-gp), an ATP binding cassette (ABC) efflux transporter (Jin et al., 2015). ABC transporters are overexpressed in HCC cells and also contribute to MDR (Ceballos et al., 2019). Indeed, SIRT1 overexpression was associated with resistance to sorafenib and other chemotherapeutic drugs in HCC cell lines (Chen et al., 2012; J. Chen et al., 2011; Liang et al., 2008).

Based on the functional role of SIRTs 1 and 2, their inhibition might be of great value in the development of new therapeutic targets in HCC. We reported that two SIRTs 1 and 2 inhibitors, cambinol and EX-527, decreased cellular viability, the number of colonies and cellular migration and increased apoptosis in 2D cultures of HCC cell lines (Ceballos et al., 2018). These compounds were also able to decrease the viability and growth of 3D cell cultures. In addition, we demonstrated that SIRT1 and SIRT2 modulation by cambinol and EX-527, as well as by silencing technology, affected the expression of P-gp and multidrug resistance-associated protein 3 (MRP3), another ABC transporter (Ceballos et al., 2018).

The aim of the present study was to analyze whether cambinol and EX-527 have the potential to enhance the response of HCC cells to sorafenib in 2D and 3D culture models. We focused particularly in assessing the impact of treatments on cellular viability, proliferation, migration, invasion and apoptosis. We also explored the effect of treatments on expression of ABC transporters in 2D cell cultures.

2. Materials and methods

2.1. Chemicals and antibodies

Sorafenib (10009644) was from Cayman Chemical (Ann Arbor, MI, USA). Cambinol (C0494) and EX-527 (E7034) drugs and anti-β-Actin (A2228) and anti-MRP3 (M0318) antibodies were obtained from Sigma-Aldrich Corp. (St. Louis, MO, USA). Anti-PCNA (sc-56), anti-P-glycoprotein (sc-55510) and anti-BCRP (sc-58222) antibodies were from Santa Cruz Biotechnology Inc. (Santa Cruz, CA, USA). Anti-Cyclin D1 antibody (ab134175) was obtained from Abcam (Cambridge, MA, USA). Anti-Ki67 antibody (PA5-19462) was obtained from Thermo Fisher Scientific (Rockford, IL, USA). Anti-MRP2 antibody (ALX-801-016) was from Enzo Life Sciences, Inc. (Farmingdale, NY, USA). All other chemicals were of the highest grade commercially available.

2.2. Studies in 2D cell cultures

2.2.1. Cell lines and treatments

The human HCC cell lines HepG2 and Huh7 were obtained from ATCC (Manassas, VA, USA) and JCRB Cell Bank (Tokyo, Japan), respectively. Cells were maintained in Dulbecco's modified Eagle's medium (DMEM) supplemented with 10% fetal bovine serum (FBS), 100 IU/ml penicillin, and 100 μg/ml streptomycin at 37°C in a humidified atmosphere of 95% O_2 and 5% CO_2. In order to inhibit SIRTs 1 and 2 activities, two inhibitors were used in combination with sorafenib, cambinol and EX-527; since they have shown promising results *in vitro* and *in vivo* as antitumor agents, alone or in combination with other drugs (Asaka et al., 2015; Bhalla and Gordon, 2016; Chen et al., 2017; Heltweg et al., 2006; Marshall et al., 2011; Portmann et al., 2013). Cambinol and EX-527 target both SIRT1 and SIRT2. However, while cambinol inhibits SIRT1 and SIRT2 with similar IC50s (IC50 SIRT1 = 56 μM; IC50 SIRT2 = 59 μM), EX-527 is much more selective for SIRT1 than for SIRT2 (IC50 SIRT1 = 0.1-1 μM; IC50 SIRT2 = 20-33 μM) (Lugrin et al., 2013). Cambinol binds to the nicotinamide binding pocket of SIRTs 1 and 2 and exhibits competitive inhibition toward the acetyl-lysine peptide substrate and noncompetitive toward NAD^+ (Heltweg et al., 2006). EX-527 binding to the nicotinamide binding pocket of SIRTs 1 and 2 requires NAD^+, alone or together with the acetyl-peptide, and the inhibition is noncompetitive

with the substrate and uncompetitive with NAD^+. EX-527 forms a complex with a coproduct of the reaction, stabilizing a closed enzyme conformation and preventing product release (Gertz et al., 2013; Napper et al., 2005).

After 24 h of attachment, cells were treated for 72 h with different doses of sorafenib to obtain dose-response curves. Alternative, in most experiments, after attachment cells were treated for 72 h with 50 μM cambinol (Camb 50); 40 μM EX-527 (EX 40); 2 μM or 1 μM sorafenib (Sfb 2 or Sfb 1) for HepG2 and Huh7 cells, respectively; and sorafenib combined with cambinol or EX-527 (combined treatments: Sfb + Camb 50 or Sfb + EX 40). All drugs were dissolved in dimethylsulfoxide (DMSO). Control (untreated) cells were incubated only with DMSO, with a final concentration in the culture medium always below 0.5%.

2.2.2. MTT assay

Cells were seeded in 96-well plates at a density of 10,000 cells/well for HepG2 and 4,000 cells/well for Huh7. After attachment, cells were treated with different doses of sorafenib or with the treatments indicated in section 2.2.1. After treatment, 3-(4,5-dimethyl-2-thiazolyl)-2,5-diphenyl-2H-tetrazolium bromide (MTT; Sigma-Aldrich Corp.) was added into the culture medium to assess its metabolization, as previously described (Ceballos et al., 2018). Absorbance of the metabolite produced from viable cells was detected at 540 nm (reference filter 650 nm) in a DTX 880 multimode detector (Beckman Coulter Inc., Fullerton, CA, USA). Results were expressed as percentage of absorbance in control cells. The half-maximal inhibitory concentration resulting in 50% cell-growth inhibition (IC50) was determined using CompuSyn software (ComboSyn, Paramus, NJ).

2.2.3. Clonogenic survival assay

Cells were seeded in 6-well plates at a density of 8,000 cells/well for HepG2 and 500 cells/well for Huh7, cultured overnight and treated for 72 h. After treatment, cells were cultured in fresh medium without drugs for 7 days. Media were replaced every 2-3 days. Finally, cell colonies were washed twice with PBS, fixed with methanol for 10 min and stained with toluidine blue (1% (W/V) in 1% (W/V) sodium borate) for 5 min. The plates were rinsed with water, air-dried, photographed and evaluated for colony estimation. Colonies were counted and relative colony formation was determined by the ratio of the average number of colonies in treated cells to the average number of colonies in control cells.

2.2.4. Western blot analysis

Cells were seeded in 6-well plates at a density of 500,000 cells/well for HepG2 and 250,000 cells/well for Huh7. After treatment, cells were washed, scrapped, collected and resuspended in homogenization buffer (250 mM sucrose, 20 mM Tris-HCl, 5 mM EDTA; pH 7.4) containing protease inhibitors to obtain total cell homogenates. The protein concentration was determined by Sedmak and Grossberg method (Sedmak and Grossberg, 1977), using bovine serum albumin (BSA) as a standard.

Equal amounts of proteins (20 µg per lane) were resolved by 8% or 12% SDS-PAGE and electroblotted onto polyvinyl difluoride (PVDF) membranes (PerkinElmer Life Sciences Inc., Boston, MA, USA). Immunoblots were blocked with PBS-10% nonfat milk, washed and incubated overnight at 4°C with primary antibodies. Finally, membranes were incubated with peroxidase-conjugated secondary antibodies and bands were detected by enhanced chemiluminescence (ECL^{TM}) detection system (Thermo Fisher Scientific). The immunoreactive bands were quantified by densitometry using the Gel-Pro Analyzer software (Media Cybernetics, Silver Spring, MD, USA). Equal loading and transference of protein was checked by detection of β-actin and by Ponceau S staining (latter data not shown) of the membranes.

2.2.5. Cell cycle analysis

Cells were seeded in 6-well plates at a density of 500,000 cells/well for HepG2 and 250,000 cells/well for Huh7 and treated the next day for 72 h. Then, cell distribution in the cell cycle was analyzed by determining the cellular DNA content by flow cytometry, as we previously described (Ferretti et al., 2019). Briefly, 1×10^6 cells were fixed with cold 70% ethanol, washed with PBS and stained with 50 µg/ml propidium iodide (Sigma-Aldrich Corp.) in a buffer solution (0.1% sodium citrate, 0.02 mg/ml RNAse, and 0.3% NP-40). Results were analyzed using WinMDi and Cylchred software.

2.2.6. Annexin V/propidium iodide assay

Cells were seeded in 6-well plates at a density of 500,000 cells/well for HepG2 and 250,000 cells/well for Huh7 and treated the next day for 72 h. After detachment of cells, apoptotic cell death was assessed by Annexin V-FITC and propidium iodide staining (FITC Annexin V Apoptosis Detection Kit II;BD Biosciences, San Jose, CA, USA) coupled to flow cytometric analysis (BD FACSAria™ II cell sorter flow cytometer, BD Biosciences), as previously described (Ceballos et al., 2018).

2.2.7. Caspase-3/7 activation assay

The activity of caspase-3/7 was determined with the CellEvent™ Caspase-3/7 Green ReadyProbes™ Reagent (Thermo Fisher Scientific). This reagent is a novel non-toxic fluorogenic substrate for activated caspases 3 and 7 and consists of a four amino acid peptide (Asp-Glu-Val-Asp: DEVD) conjugated to a nucleic acid binding dye. DEVD is the consensus sequence cleaved by caspases 3 and 7 in their substrates. This cell-permeant substrate is intrinsically non-fluorescent, because the DEVD peptide inhibits the ability of the dye to bind to DNA. After activation of caspase-3 or caspase-7 in apoptotic cells, the DEVD peptide is cleaved, enabling the dye to bind to DNA and produce a bright, fluorogenic response with absorption/emission maxima of ~502/530 nm.
Cells were seeded in 96-well plates at a density of 12,000 cells/well for HepG2 and 4,000 cells/well for Huh7. After treatment, 10 µl of reagent was added per well and cells were incubated for 30 min at 37°C in a humidified atmosphere of 95% O_2 and 5% CO_2. Cells were observed using an inverted fluorescence microscope (Zeiss Axiovert 25; Zeiss, Oberkochen, Germany) connected to a digital camera (Nikon Coolpix 990; Nikon, Tokyo, Japan).

2.2.8. Wound healing assay

Cells seeded at 3×10^6/well for HepG2 and 1×10^6/well for Huh7 were cultured in 6-well plates. After 24 h, cells were wounded by dragging a 200 µl pipette tip through the confluent monolayer, washed with PBS and treated for 24 h to allow migration. Images of wounds in the same field were captured when the scrape wound was introduced (0 h) and after 24 h of wounding (18 fields/well) using an inverted microscope (Zeiss Axiovert 25) connected to a digital camera (Nikon Coolpix 990). The area and height of the wound were determined using ImageJ software (NIH) and the healing width was calculated as the area to height ratio. The migrated distance (µm) was then calculated with the formula = wound width at 0 h - wound width at 24 h, and expressed as percentage relative to control cells.

2.2.9. Transwell cell invasion assay

Invasion assay was performed using transwell chambers with 8 µm pore size polyester membrane filters (Biofil, Beijing, China) precoated with ECM gel (Sigma-Aldrich Corp.). Huh7 cells in DMEM containing 1% FBS were harvested and reseeded in the upper chambers at a density of 50,000 cells per well, and the lower chambers were filled with complete DMEM medium containing 10% FBS. Treatments were added to upper and lower chambers. After 48 h, ECM gel and remaining cells (non-invasive cells) on the top surface of the membrane in the upper chambers were removed using a cotton swab whereas cells that invaded and remained attached to the

bottom surface of the membrane were fixed and stained in the same way as for colonies. For quantification, cells in 15 randomly selected microscopic fields were photographed and counted using an inverted microscope. Cells that invaded the lower chambers were expressed as percentage relative to control cells.

2.3. Studies in 3D cell cultures (spheroids)

Three-dimensional cell culture models such as spheroids closely mimic the main features of human solid tumors and manifest an elevated MDR compared to 2D cell cultures thus representing valuable *in vitro* models for the preclinical evaluation of anticancer drug treatments (Mehta et al., 2012; Vinci et al., 2012).

2.3.1. Generation of spheroids and treatments

Spheroids from HCC cells were obtained by liquid overlay technique in 96-well plates as previously described (Ceballos et al., 2018). Briefly, wells were coated with a mixture of 3% agarose in water (W/V): DMEM (1:1) and 2 h later HepG2 and Huh7 cells were seeded at a density of 1,500 cells/well. Culture conditions were the same as for 2D cell cultures. Spheroids were formed after an initiation interval of 4 days (0 h) and then treated until day 7 (72 h) with different concentrations of sorafenib (APH and spheroid growth delay assays) or with 50 μM cambinol (Camb 50); 80 μM or 40 μM EX-527 (EX 80 or EX 40) for HepG2 and Huh7 cells, respectively; 4 μM or 2 μM sorafenib (Sfb 4 or Sfb 2) for HepG2 and Huh7 cells, respectively; and sorafenib combined with cambinol or EX-527 (combined treatments: Sfb + Camb or Sfb + EX). All drugs were dissolved in DMSO. Control (untreated) spheroids were incubated only with DMSO, with a final concentration in the culture medium always below 0.5%. Spheroids were treated by replacing 50% of the supernatant by fresh medium supplemented with drugs prepared at twice of the desired doses.

Techniques to avoid spheroids disaggregation and thus to study the behavior of whole spheroids were chosen. In this way, we were able to visualize drug response in different regions of spheroids.

2.3.2. Spheroid viability and growth: acid phosphatase and spheroid growth delay assays

Spheroids were treated for 72 h with different doses of sorafenib or with the treatments indicated in section 2.3.1. and then the acid phosphatase (APH) assay was performed for viability assessment, according to the protocol of Friedrich et al. (Friedrich et al., 2007). The substrate *p*-nitrophenyl phosphate was kindly provided by Wiener Lab. (Buenos Aires, Argentina). Absorption of *p*-nitrophenol at 405 nm was measured in a DTX 880 multimode

detector. Results were expressed as percentage of absorbance in control cells. The IC50 was determined using CompuSyn software.

For assessing the volume of 3D cell cultures, spheroids images were captured before (day 4; 0 h) and after (day 7; 72 h) treatments using an inverted microscope (Zeiss Axiovert 25) connected to a digital camera (Nikon Coolpix 990) and diameters were determined using ImageJ software. Spheroids diameters at the onset of treatment were close to 400 - 500 µm, as recommended (Friedrich et al., 2009; Vinci et al., 2012). In this regard, spheroids with diameters larger than 400 µm follow a concentrically layered structure consisting of an apoptotic/necrotic core surrounded by a viable layer of quiescent cells and an outer ring of proliferating cells (Hirschhaeuser et al., 2010; Mehta et al., 2012). This cellular heterogeneity is similar to that of avascular microregions of tumors (Hirschhaeuser et al., 2010; Mehta et al., 2012) and, in the same way, the concentration of drugs, oxygen and nutrients decreases in the distant inner cells of spheroids contributing to MDR (Mehta et al., 2012). Spheroids volumes were calculated before and after treatments using the equation: $V = (4/3)\pi R^3$; $R = (D1 + D2)/4$, where D1 and D2 are the maximal diameters of spheroids measured in the rectangular direction. Results were expressed as the percentage of volume at 72 h vs. 0 h (Ceballos et al., 2018).

2.3.3. Immunofluorescent analysis of spheroid sections

To obtain frozen sections, spheroids were harvested after treatments and transferred to Eppendorf tubes (~20 spheroids/tube), rinsed twice with PBS and fixed in 4% paraformaldehyde for 1 h. After fixation, spheroids were rinsed twice with PBS, transferred to cryomolds and embedded in Cryoplast compound (Biopack, Buenos Aires, Argentina) for cryostat sectioning (Microm HM 500; Zeiss). Sections of 8 µm were obtained, mounted onto slides and stored at -70ºC until used. For immunostaining, sections were permeabilized and blocked with 3% BSA and 0.3% Triton X-100 in PBS for 20 min and then incubated overnight at 4°C with primary antibodies. After washes in PBS, sections were incubated with appropriate Cy2- or Cy3-conjugated secondary antibodies (Jackson ImmunoResearch Laboratory, Inc., West Grove, PA, USA) for 1 h, washed, incubated for nuclei staining with 4′,6-diamidino-2-phenylindole (DAPI; Thermo Fisher Scientific) and mounted with ProLong (Thermo Fisher Scientific). Fluorescence was detected by using confocal microscopy (Nikon C1SiR with inverted microscope Nikon TE200E and Zeiss LSM880). Images were obtained with the confocal software and then processed using ImageJ software. To ensure comparable staining and image capture performance for control and treated cells, all groups were processed in parallel. For quantification, the number of positive cells for Ki-67, PCNA and cyclin D1 and the total number of cells (DAPI-positive nuclei) per section of spheroid were counted

using the ITCN (Image-based Tool for Counting Nuclei) plugin of the ImageJ software. The total number of Ki-67-, PCNA- and cyclin D1-positive stained cells per section of spheroid and the fraction of Ki-67-, PCNA- and cyclin D1-positive cells per total number of cells per section of spheroid (proliferation marker positive cells/DAPI-positive cells) was determined in at least 8 sections of spheroids from two independent experiments and data was expressed as percentage relative to the control group.

2.3.4. Caspase-3/7 activation assay

As for 2D cultures, the activity of caspase-3/7 was determined with the CellEvent™ Caspase-3/7 Green ReadyProbes™ Reagent. This reagent was validated in fresh whole spheroids and showed no toxicity for cultures (Mittler et al., 2017). After treating spheroids the same protocol used for 2D cultures was applied (section 2.2.7.), except that 20 µl of reagent was added per well and spheroids were incubated for 1 h prior to microscopic observation. Fluorescence intensity was measured using ImageJ software and data was expressed as percentage relative to control cells.

2.3.5. Spheroid migration assay

Migration was assessed in whole spheroids based on the protocol by Xu et al. (Xu et al., 2012), with slight modifications. Spheroids from the Huh7 cell line were obtained and photographed before treatment (day 4; 0 h) using an inverted microscope connected to a digital camera. Spheroids were then transferred to 96-well plates without base-coated agarose to allow their adhesion to wells. Under these conditions, spheroids are able to disassemble and release cells that have the ability to migrate. Once transferred, spheroids were treated in serum free medium to attenuate cellular proliferation and the process of migration was followed obtaining images at 24, 48 and 72 h, using an inverted microscope. Diameters were determined using ImageJ software at 0, 48 and 72 h and areas were calculated using the equation: $A = 4\pi R^2$; $R = (D1 + D2)/4$, where D1 and D2 are the maximal diameters of spheroids measured in the rectangular direction. The migration capability was then estimated by relativizing the area covered by the spheroid together with the cells that have migrated from it at 48 or 72 h to the initial area of the spheroid at 0 h and expressing results as percentage of the control group (Vinci et al., 2012).

2.4. Statistical analysis

Results were expressed as mean ± S.E.M. Significance in differences was tested by one-way ANOVA followed by Tukey test. Differences were considered significant when the P value was < 0.05.

3. Results

3.1. The presence of cambinol or EX-527 increments the cytotoxic effect of sorafenib

Two-dimensional cultures were treated with different doses of sorafenib for 72 h. As expected, sorafenib reduced cellular viability in a dose-dependent manner compared with control cells in HepG2 and Huh7 cell lines (Fig. 1 A). The IC50 (µM) for sorafenib was 4.32 ± 0.54 in HepG2 cells and 2.88 ± 0.38 in Huh7 cells. Based on this result, we choose one dose of sorafenib for each HCC cell line for further studies; 2 µM (Sfb 2) for HepG2 and 1 µM (Sfb 1) for Huh7 cells. These doses generated a small but significant reduction of cell viability (below the IC50 values) that was of similar extent in both cell lines.

Next, we analyzed if cambinol and EX-527 were capable of modifying the cytotoxic effect of sorafenib in 2D cultures. Doses for cambinol and EX-527 were chosen based on the results from our previous study and were the same for both cell lines; 50 µM for cambinol (Camb 50) and 40 µM for EX-527 (EX 40) (Ceballos et al., 2018). The selection was also based on the fact that cambinol and EX-527 were able to inhibit SIRT1 and SIRT2 at these doses (Ceballos et al., 2018; Lugrin et al., 2013). As seen in Fig. 1 B, the addition of cambinol or EX-527 as a combined treatment (Sfb + Camb 50 or Sfb + EX 40) significantly raised sorafenib cytotoxicity in 2D cultures of both HCC cell lines. The clonogenic assay confirmed the toxicity of the different treatments and was in accordance with MTT results as the lowest percentages of colonies were obtained with the combined treatments (Fig. 1 C).

In the case of 3D cell cultures, data show a dose-dependent reduction of spheroid viability after sorafenib treatment when compared with untreated spheroids from both cell lines (Fig. 2 A). The IC50 values (µM) for sorafenib were 11.70 ± 0.60 in HepG2 and 8.17 ± 1.01 in Huh7 spheroids. Importantly, these values were significantly higher than those from the respective 2D cultures (Fig. 1 A), indicating a lower sensitivity of spheroids to sorafenib treatment ($P < 0.05$ vs. 2D).

Following the same strategy used in 2D cultures, we choose one dose of sorafenib for each HCC cell line for further studies; 4 µM (Sfb 4) for HepG2 and 2 µM (Sfb 2) for Huh7 spheroids. As shown in Fig. 1, these doses generated a small but significant reduction of cell viability that was comparable between cell lines and the doses were higher than those chosen for 2D cultures due to the increased resistance of spheroids to sorafenib. Although it was desirable to use the same dose of cambinol (Camb 50) and EX-527 (EX 40) for treating the spheroids of

both cell lines, we had to increase the dose of EX-527 in 3D cultures from HepG2 cells (80 μM; EX 80) due to the high resistance of HepG2 spheroids to this drug (Ceballos et al., 2018). The addition of cambinol or EX-527 as a combined treatment significantly increased sorafenib cytotoxicity in spheroids from both HepG2 and Huh7 cells (Fig. 2 B).

3.2. SIRTs inhibitors lead to a diminution of cellular proliferation during sorafenib treatment

To analyze if the addition of SIRTs inhibitors during sorafenib treatment affects the proliferation of 2D cultures, we quantified the levels of proliferating cell nuclear antigen (PCNA) and cyclin D1 proteins by western blot. Whereas Cambinol and EX-527 were able to reduce PCNA and cyclin D1 protein levels, sorafenib failed to diminish the levels of these proteins (Fig. 3 A, B). However, when sorafenib was combined with the inhibitors a significant reduction was achieved in both HCC cell lines (Fig. 3 A, B). Next, we studied the effect of treatments on cell cycle progression in 2D cultures. Although changes were small, we observed that the population of cells in G0/G1 was increased and that of S was reduced by treatments with the greatest variations obtained with the combined treatments (Fig. 3 C). No significant effects were registered in the population of cells in G2/M with treatments (data not shown).

As a measure of proliferation in 3D cultures, we calculated the volume of the spheroids before and after treatments (Vinci et al., 2012). Sorafenib alone induced a concentration-dependent growth inhibition in HepG2 and Huh7 spheroids (Fig. 4 A). As shown in Fig. 4 (B, C), cambinol and EX-527 exacerbated the effect of sorafenib on volume reduction of HepG2 and Huh7 spheroids.

To further explore the antiproliferative capacity of treatments in 3D cultures we evaluated the expression of Ki-67, PCNA and cyclin D1 proteins by immunofluoresce in frozen sections of spheroids. As shown in Fig. 5 (A, B), Ki-67, PCNA and cyclin D1 staining was localized in the peripheral layers of sections of spheroids. Compared to control spheroids, treated spheroids from both cell lines generally exhibited a reduction in the thickness of the peripheral ring corresponding to cells that were positive for the proliferation markers. In HepG2, combined treatments reduced proliferation in spheroid cultures compared to sorafenib treatment as quantified by Ki-67, PCNA and cyclin D1 staining (Fig. 5 C-E). The total number of proliferation marker-positive cells per spheroid was lower in HepG2 spheroids subjected to combined treatments. Nevertheless, as a consequence of the lower number of total cells in treated spheroids, in some cases, the fraction of positive cells was not significantly diminished. Only the presence of cambinol in sorafenib-treated spheroids diminished the number of Ki-67- and PCNA-positive cells when compared to sorafenib treatment in Huh7 spheroids (Fig. 5 C, D). In the case of the

combined treatment with EX-527 and with both combined treatments for cyclin D1 staining, only a non-significant tendency to reduction of the number of positive cells was found in Huh7 regarding to sorafenib-treated spheroids (Fig. 5 C-E).

3.3. Cambinol and EX-527 raise the apoptotic effect of sorafenib

Cytometric annexin V-PI assay at 72 h demonstrated that both SIRTs 1 and 2 inhibitors incremented the apoptosis observed after sorafenib treatment in 2D cultures from HepG2 and Huh7 cells (Fig. 6 A). Nevertheless, whereas the combined treatment with Camb 50 incremented early (Annexin V+/PI-) and late (Annexin V+/PI+) apoptosis when compared to sorafenib alone, only early apoptosis was increased with the addition of EX 40 in the combined treatment. The same behavior was observed when treating HCC cells only with SIRTs inhibitors; i.e., Camb 50 incremented early and late apoptosis while EX 40 raised only early apoptosis, compared with untreated cells (Fig. 6 A). No changes were found with treatments in primary necrotic death as assessed by determination of the Annexin V-/PI+ ratio (data not shown).

We evaluated caspase-3/7 activity as an alternative method to corroborate the induction of apoptosis in the presence of treatments in 2D cultures. As seen in Fig. 6 B, cambinol, EX-527 and sorafenib treatments lead to an increment of caspase-3/7 staining intensity and the number of caspase-3/7 positive (apoptotic) cells when compared with control cells. In concordance with the annexin V-PI assay, combined treatments produce the largest increments in caspase-3/7 activity (Fig. 6 B). Also, according to the cytotoxic effect of treatments, a reduction of cell density was observed in cells treated with cambinol, EX-527 and sorafenib that became more noticeable after the combined treatments (Fig. 6 B).

In 3D cultures, we also used the CellEvent™ Caspase-3/7 Green ReadyProbes™ Reagent to evaluate apoptosis. As shown in Fig. 7, control spheroids showed a CellEvent-positive central region. More interesting, cambinol, EX-527 and sorafenib treatments resulted in an increase of caspase-3/7 staining intensity in spheroids core regions, with the largest caspase-3/7 activation observed upon the combined treatments (Fig. 7).

3.4. The addition of SIRTs inhibitors during sorafenib treatment decreases cellular migration and invasiveness

To reduce potential proliferation or apoptosis effects we performed wound healing assays in 2D cultures within a short time period (24 h), before the doubling time of HepG2 and Huh7 cells (Sun et al., 2011). Additionally, we performed MTT assays to check the effect of treatments on cytotoxicity at 24 h. As seen in Fig. 8 A, B, despite the fact that the dose used for sorafenib did not affect cellular migration, combined treatments were able to

reduce the migration in 2D cultures. Since cell viability was always > 90% as detected in MTT assays (data not shown), we can infer that inhibition of migration by combined treatments is not due to cytotoxic effects.

In view of the alteration of cell migration in 2D cultures, we evaluated if invasiveness may be also affected. Experiments using Huh7 cells showed that cambinol, EX-527 and sorafenib treatments led to a decrease in cellular invasion and that the addition of SIRTs 1 and 2 inhibitors to sorafenib treated-cells exacerbated the effect of non-combined treatments (Fig. 8 C).

Then, we analyzed migration in 3D cultures using whole spheroids from Huh7 cells. Although no cellular migration was observed at 24 h post-treatment (data not shown), all treatments, except the one with sorafenib alone, significantly decreased the migration of spheroids at 48 and 72 h (Fig. 9).

3.5. Cambinol and EX-527 affect the expression of some ABC transporters during sorafenib treatment

We explored the effect of adding cambinol or EX-527 to sorafenib treatment on the expression of P-gp, MRP3, BCRP and MRP2 in 2D cultures from HepG2 and Huh7 cells. As shown in Fig. 10, cambinol alone decreased the expression of P-gp and MRP3 in HepG2 cells but augmented the expression of all the studied transporters in Huh7 cells. P-gp expression decreased in HepG2 cells but augmented in Huh7 cells in response to EX-527. The expression of MRP3 and BCRP was reduced and a trend to decrease in MRP2 expression was found after the treatment with EX-527 in both HCC cell lines. Additionally, sorafenib induced an increase in MRP3 expression and a trend to increase the expression of some of the other transporters, in both cell lines. In HepG2 cells, combined treatments diminished the expression of P-gp and MRP3 with respect to sorafenib treatment and, in the case of P-gp, the levels found were even lower than those of the control group. Also, the expression of BCRP decreased with the presence of EX-527 in the combined treatment in this cell line. In the Huh7 cell line, the presence of cambinol in the combined treatment raised the expression of all the studied transporters. Finally, in Huh7 cells, the presence of EX-527 in the combined treatment augmented the expression of P-gp but was able to reduce the level of MRP3 and BCRP compared with sorafenib treatment.

4. Discussion

There is an urgent need to improve HCC sensitivity to sorafenib. The aim of this study was to analyze the impact of two SIRTs 1 and 2 inhibitors on sorafenib-treated tumor cells, focused on specific features associated with malignancy.

The IC50 values found for sorafenib in the cytotoxic studies were similar to those reported in the literature and were within the clinically relevant concentration range for this drug (K. F. Chen et al., 2011; Cui et al., 2014; Jiang et al., 2015; Khawar et al., 2018; Lin et al., 2020; Liu et al., 2006). SIRTs inhibitors exacerbated the effects of sorafenib on the viability of 2D and 3D cultures of HepG2 and Huh7 cells. To our knowledge, there are no studies showing the effects of combination of sorafenib with cambinol, EX-527 or other SIRTs 1 and 2 inhibitors, although it is worth mentioning that Chen et al. (Chen et al., 2012) demonstrated that SIRT1 overexpression promoted resistance to sorafenib in the HCC cell line SK-Hep1.

It was reported that cambinol and EX-527 (Holloway et al., 2010; Kang et al., 2018; Ponnusamy et al., 2014) as well as the knockdown of SIRT1 and SIRT2 (Ponnusamy et al., 2014; Pruitt et al., 2006) reduced the expression of PCNA and cyclin D1 in diverse cell lines. In addition, Chen et al. (Chen et al., 2019) showed that Ki-67 protein level greatly decreased in SIRT1 knockdown and EX-527-treated glioma tumors established in nude mice. Regarding SIRT2, one work demonstrated that Ki-67 expression was increased after SIRT2 overexpression in a myoblast cell line (Wu et al., 2014). Specifically in HCC cells, it was only described the reduction of PCNA and cyclin D1 expression after SIRT1 silencing (Bae et al., 2014); and SIRT1 expression was positively correlated with Ki-67 expression in human HCC tissues (Jang et al., 2012). In our study, combined treatments were effective in decreasing the proliferation of 2D cultures and 3D cultures treated with sorafenib in the presence of SIRTs inhibitors showed a greater fall in spheroid growth. In addition, the strongest reduction in proliferative cells was observed in sections obtained from HepG2 spheroids treated with sorafenib in the presence of SIRTs inhibitors, consistent with the smallest volumes of spheroids and the largest decrease in cellular proliferation found under this condition. In Huh7 spheroids, the presence of cambinol in the combined treatment was capable of diminishing the number of Ki-67- and PCNA-positive cells when compared to sorafenib treatment. To our knowledge, this is the first work aimed to explore the effect of sorafenib or SIRTs inhibitors on these proliferation markers in 3D cultures.

The gradient of proliferation characteristic of 3D cultures (Mehta et al., 2012) was clearly visible in sections of spheroids from both cell lines immunostained for Ki-67, PCNA and cyclin D1. This pattern of staining was already described for Ki-67 and PCNA in sections obtained from spheroids of HCC cell lines (Baulies et al., 2018; Jung et al., 2017). This is the first work describing the expression of cyclin D1 in 3D cell cultures from HCC cells. Laurent et al. (Laurent et al., 2013) showed that spheroids from pancreatic cancer cells displayed an expression pattern of cyclin D1 that mirrored the proliferation gradient of 3D cultures.

It is interesting to note that Ki-67, PCNA and cyclin D1 are prognostic biomarkers related to tumor growth rate and poor prognosis in HCC (Burkhart et al., 2017). In this regard, the fact that combined treatments decreased the expression of these proliferation markers in 3D cell cultures could be of extreme value in identifying clinically relevant therapies with a higher predictive value for clinical outcome (Langhans, 2018).

It was described that cambinol lead to a G0/G1 arrest in HepG2 cells (Portmann et al., 2013) and that EX-527 also caused cell cycle arrest at G0/G1 in other cancer cell lines (Peck et al., 2010; Singh et al., 2015). In our work, combined treatments presented more growth arrest in G1/G0 phase of cell cycle regarding sorafenib alone.

In the current study, we were able to detect caspase-3/7 staining in the core region of whole control spheroids consistent with apoptosis induction within the nutrient deprived spheroid core (Mehta et al., 2012). Interestingly, 2D and 3D cultures treated with sorafenib in the presence of SIRTs 1 and 2 inhibitors exhibited more apoptosis than cultures treated only with sorafenib. Although there are no studies evaluating the impact of SIRTs 1 and 2 inhibitors on sorafenib apoptosis, Garten et al. (Garten et al., 2019) proposed recently that SIRT1 overexpression could be an underlying mechanism of sorafenib resistance in HCC since transient overexpression of SIRT1 decreased sorafenib-induced apoptosis in Huh7 cells.

It was reported that SIRTs 1 and 2 knockdowns significantly reduced migration and invasion in HCC cell lines and HCC tumor metastasis *in vivo* (Chen et al., 2013; Hao et al., 2014; Li et al., 2016). In our study, the addition of SIRTs 1 and 2 inhibitors potentiated the effect of sorafenib to inhibit cellular migration and invasion.

Sorafenib induced the expression of MRP3 in 2D cultures of both HCC cell lines. Even though HCC cell lines resistant to sorafenib have more MRP3 expression than the corresponding parental cells (Chow et al., 2013; Tomonari et al., 2016), the effect of sorafenib on MRP3 expression in sensitive HCC cells has not been studied. Combined treatments showed less expression of P-gp and MRP3 than the individual treatment with sorafenib in HepG2 cells. In addition, the expression of BCRP decreased with the addition of EX-527 to the combined treatment in this cell line. In accordance with our previous study (Ceballos et al., 2018), cambinol and EX-527 reduced P-gp and MRP3 expression in HepG2 cells. In these cells, we also found that EX-527 was able to reduce BCRP protein levels. In line with our results, the inhibitory effect of EX-527 on P-gp expression was already reported in non-HCC cancer cell lines (H.-B. Kim et al., 2015; Zhu et al., 2012) and Wen et al. (Wen et al., 2020) showed recently that EX-527 inhibited the expression of MRP3 and raised 5□Fluorouracil sensitivity in 5□Fluorouracil-resistant HCC tumors established in nude mice. Additionally, BCRP expression was remarkably inhibited by transfection of non-HCC cancer cell lines with SIRT1 siRNAs (H. B. Kim et al., 2015; Wang et al., 2016). Although one study describes that the SIRTs inhibitor nicotinamide reduced the expression of MRP2 in

breast cancer cells (Choi et al., 2013), we only found a trend to decrease in MRP2 expression in EX-527-treated cells. In contrast to HepG2 cells, treatment with cambinol, alone or in combination with sorafenib, induced the expression of all the studied transporters in Huh7 cells. Even though EX-527 increased the expression of P-gp, this drug was able to diminish the expression of MRP3 and BCRP in Huh7 cells. In accordance with this, the addition of EX-527 to the combined treatment augmented the expression of P-gp and reduced the expression of MRP3 and BCRP compared with sorafenib treatment in these cells. Although we do not know the mechanism involved in the dissimilar behavior between HCC cell lines, we believe that the p53 suppressor protein could play a key role. HepG2 cells express a wild-type form of p53 whereas Huh7 cells express a mutant form of this protein (Hsieh et al., 2003). It was observed that whereas wild-type p53 generally represses MDR1 promoter, some mutants of p53 stimulate its activity (Zastawny et al., 1993). In fact, certain p53 mutants upregulated P-gp expression and activity in cancer cells, including in a HCC cell line (Chan and Lung, 2004; Tsou et al., 2015). This mechanism could be also responsible for the dissimilar behavior between P-gp and MRP3 and BCRP in Huh7 cells when only considering the specific SIRTs 1 and 2 inhibitor EX-527, since it was described that cambinol lacks selectivity and targets more than SIRT1 and SIRT2 (Lugrin et al., 2013) and thus could be activating alternative pathways to modulate the expression of ABC transporters. Moreover, despite studies are still needed regarding MRP3, it was reported *in vitro* and *in vivo* that sorafenib is moderately transported by P-gp, being a weak substrate of this ABC transporter, and more efficiently by BCRP (Gnoth et al., 2010; Lagas et al., 2010). In this way, Gnoth and col. (Gnoth et al., 2010) conclude that it is unlikely that P-gp has a major effect on the plasma concentrations of sorafenib in humans. On the other hand, in HCC cell lines, it was showed that BCRP mediated the efflux of sorafenib (Huang et al., 2013) and that MRP3 and BCRP are involved in sorafenib resistance (Huang et al., 2013; Tomonari et al., 2016; Wang et al., 2020). In spite that resistance mechanisms underlying the impaired sensitivity to sorafenib are still elusive and the role of ABC transporters in this resistance remains to be better elucidated (Beretta et al., 2017), it is probably that BCRP and MRP3 are being part of the mechanism that takes place during SIRTs 1 and 2 inhibition to enhance the response of HCC cells to sorafenib. Studies with SIRTs 1 and 2 inhibitors are still missing in sorafenib-resistant cells to better elucidate the role of ABC transporters in sorafenib resistance. Conversely, uncontrolled cell proliferation due to defects throughout cell cycle progression and apoptosis resistance are widely accepted characteristic of tumor cells and reported mechanisms of sorafenib therapy failure (Niu et al., 2017). Thus, mechanisms related to the modulation of PCNA, cyclin D1, Ki-67 and caspase-3/7 proteins by SIRTs 1 and 2 inhibitors, would be

implicated in enhancing the response of HCC cells to sorafenib as well. Additionally, modulation of p53 and FoxO1 acetylation levels by cambinol and EX-527 treatments (Ceballos et al., 2018) could also be involved. Finally, it is worthy to highlight our results in 3D cultures, as spheroids are considered good predictors of the therapeutic response in patients (Langhans, 2018). In fact, many treatments are expected to lose efficacy when tested in 3D cultures (Hirschhaeuser et al., 2010). Thus, a potentially relevant observation in our study was that the beneficial effects of adding cambinol or EX-527 to sorafenib-treated cells were maintained when moving from 2D to 3D cultures, suggesting that the inhibition of SIRTs 1 and 2 could be effective in sensitizing HCC cells to sorafenib treatment *in vivo*. In this connection, cambinol and EX-527 were already tested *in vivo*, being effective in inhibiting tumor growth in murine models of cancer and, at the same time, well tolerated by mice without induction of weight loss or adverse effects (Asaka et al., 2015; Chen et al., 2017; Heltweg et al., 2006; Marshall et al., 2011; Portmann et al., 2013). In fact, cambinol impaired HCC growth in an orthotopic xenograft model and displayed no signs of hepatic damage or impairment of the regenerative capacity of normal liver in response to partial hepatectomy (Portmann et al., 2013). Furthermore, EX-527 was tested in phase I and II clinical trials for the treatment of Huntington's disease (a neurodegenerative disorder) and was found to be safe and well tolerated by patients (Süssmuth et al., 2015) and by healthy volunteers as well (Westerberg et al., 2015). Although more research is still necessary in order to evaluate the safety of combining SIRTs inhibitors with chemotherapeutic agents, findings presented in this manuscript shed some light on the importance of this type of research at the preclinical as well as the clinical levels.

5. Conclusions

This manuscript described that cambinol and EX-527 enhanced the response of HCC cells to sorafenib treatment. As PCNA, cyclin D1 and Ki-67 are closely associated with cell proliferation and caspase-3/7 orchestrate apoptosis, their modulation in the presence of SIRTs 1 and 2 inhibitors likely play an important role in enhancing the response of HCC cells to sorafenib treatment. The presence of EX-527, a specific SIRTs 1 and 2 inhibitor, was able to reduce MRP3 and BCRP expression in sorafenib-treated HCC cells, suggesting that modulation of ABC transporters may be involved, at least in part, in the beneficial effects of combined treatments. Treatments were still effective in 3D cultures yielding results with higher predictive value for clinical outcome and thus providing a rationale for clinically exploring the use of SIRTs 1 and 2 inhibitors in HCC therapy to sensitize cells to sorafenib. At the same time, since the addition of SIRTs 1 and 2 inhibitors to sorafenib treatment incremented its efficacy, this could allow to reduce the dose of sorafenib, which ultimately

will impact in the reduction of appearance of adverse effects and in the quality of life of patients with HCC under therapy.

Declaration of interest

None to declare

Acknowledgements

We would like to express our gratitude to Mara J. Ojeda (CONICET) for her technical assistance in cytometric analyses, to Alejandra Martínez and Diego H. Parenti (Área Morfología, Facultad de Ciencias Bioquímicas y Farmacéuticas) for cryostat sectioning of 3D cultures, to José M. Pellegrino (IFISE-CONICET), Andrés Tome (IFISE-CONICET) and Rodrigo Vena (IBR-CONICET) for their technical assistance in confocal microcopy, to M. Cecilia Larocca for her assistance with the immunofluorescent analysis of spheroid sections and to Eugenia Carmeli Barberis for her kind help with western blot experiments. We would also like to thank Instituto Nacional del Cáncer (INC) for the research fellowship awarded to Carla B. Delprato.

Funding

This work was supported by Agencia Nacional de Promoción Científica y Tecnológica (ANPCyT; PICT 2014-2596, MP Ceballos); Agencia Santafesina de Ciencia, Tecnología e Innovación (ASaCTeI; Programas de Promoción de las Actividades Científicas Tecnológicas y de Innovación n° 2010-167-14, MC Carrillo); and Consejo Nacional de Investigaciones Científicas y Técnicas (CONICET; P-UE 2016-0089, IFISE-CONICET).

References

Asaka, R., Miyamoto, T., Yamada, Y., Ando, H., Mvunta, D.H., Kobara, H., Shiozawa, T., 2015. Sirtuin 1 promotes the growth and cisplatin resistance of endometrial carcinoma cells: A novel therapeutic target. Lab. Investig. 95, 1363–1373. https://doi.org/10.1038/labinvest.2015.119

Bae, H.J., Noh, J.H., Kim, J.K., Eun, J.W., Jung, K.H., Kim, M.G., Chang, Y.G., Shen, Q., Kim, S.J., Park, W.S., Lee, J.Y., Nam, S.W., 2014. MicroRNA-29c functions as a tumor suppressor by direct targeting oncogenic SIRT1 in hepatocellular carcinoma. Oncogene 33, 2557–2567. https://doi.org/10.1038/onc.2013.216

Baulies, A., Montero, J., Matías, N., Insausti, N., Terrones, O., Basañez, G., Vallejo, C., de La Rosa, L.C.,

Martinez, L., Robles, D., Morales, A., Abian, J., Carrascal, M., Machida, K., Kumar, D.B.U., Tsukamoto, H., Kaplowitz, N., Garcia-Ruiz, C., Fernández-Checa, J.C., 2018. The 2-oxoglutarate carrier promotes liver cancer by sustaining mitochondrial GSH despite cholesterol loading. Redox Biol. 14, 164–177. https://doi.org/10.1016/j.redox.2017.08.022

Beretta, G.L., Cassinelli, G., Pennati, M., Zuco, V., Gatti, L., 2017. Overcoming ABC transporter-mediated multidrug resistance: The dual role of tyrosine kinase inhibitors as multitargeting agents. Eur. J. Med. Chem. https://doi.org/10.1016/j.ejmech.2017.07.062

Bhalla, S., Gordon, L.I., 2016. Functional characterization of NAD dependent de-acetylases SIRT1 and SIRT2 in B-Cell Chronic Lymphocytic Leukemia (CLL). Cancer Biol. Ther. 17, 300–9. https://doi.org/10.1080/15384047.2016.1139246

Burkhart, R.A., Ronnekleiv-Kelly, S.M., Pawlik, T.M., 2017. Personalized therapy in hepatocellular carcinoma: Molecular markers of prognosis and therapeutic response. Surg. Oncol. https://doi.org/10.1016/j.suronc.2017.01.009

Ceballos, M.P., Decándido, G., Quiroga, A.D., Comanzo, C.G., Livore, V.I., Lorenzetti, F., Lambertucci, F., Chazarreta-Cifre, L., Banchio, C., Alvarez, M. de L., Mottino, A.D., Carrillo, M.C., 2018. Inhibition of Sirtuins 1 and 2 Impairs Cell Survival and Migration and Modulates the Expression of P-glycoprotein and MRP3 in Hepatocellular Carcinoma Cell Lines. Toxicol. Lett. 289, 63–74. https://doi.org/10.1016/j.toxlet.2018.03.011

Ceballos, M.P., Rigalli, J.P., Cere, L.I., Semeniuk, M., Catania, V.A., Ruiz, M.L., 2019. ABC Transporters: Regulation and Association with Multidrug Resistance in Hepatocellular Carcinoma and Colorectal Carcinoma. Curr. Med. Chem. 26, 1224–1250. https://doi.org/10.2174/0929867325666180105103637

Chan, K.-T., Lung, M.L., 2004. Mutant p53 expression enhances drug resistance in a hepatocellular carcinoma cell line. Cancer Chemother. Pharmacol. 53, 519–26. https://doi.org/10.1007/s00280-004-0767-4

Chen, G., Zhang, B., Xu, H., Sun, Y., Shi, Y., Luo, Y., Jia, H., Wang, F., 2017. Suppression of Sirt1 sensitizes lung cancer cells to WEE1 inhibitor MK-1775-induced DNA damage and apoptosis. Oncogene 36, 6863–6872. https://doi.org/10.1038/onc.2017.297

Chen, H.-C., Jeng, Y.-M., Yuan, R.-H., Hsu, H.-C., Chen, Y.-L., 2012. SIRT1 promotes tumorigenesis and resistance to chemotherapy in hepatocellular carcinoma and its expression predicts poor prognosis. Ann. Surg. Oncol. 19, 2011–9. https://doi.org/10.1245/s10434-011-2159-4

Chen, H., Lin, R., Zhang, Z., Wei, Q., Zhong, Z., Huang, J., Xu, Y., 2019. Sirtuin 1 knockdown inhibits glioma

cell proliferation and potentiates temozolomide toxicity via facilitation of reactive oxygen species generation. Oncol. Lett. 17, 5343–5350. https://doi.org/10.3892/ol.2019.10235

Chen, J., Chan, A.W.H., To, K.-F., Chen, W., Zhang, Z., Ren, J., Song, C., Cheung, Y.-S., Lai, P.B.S., Cheng, S.-H., Ng, M.H.L., Huang, A., Ko, B.C.B., 2013. SIRT2 overexpression in hepatocellular carcinoma mediates epithelial to mesenchymal transition by protein kinase B/glycogen synthase kinase-3β/β-catenin signaling. Hepatology 57, 2287–98. https://doi.org/10.1002/hep.26278

Chen, J., Jin, R., Zhao, J., Liu, J., Ying, H., Yan, H., Zhou, S., Liang, Y., Huang, D., Liang, X., Yu, H., Lin, H., Cai, X., 2015. Potential molecular, cellular and microenvironmental mechanism of sorafenib resistance in hepatocellular carcinoma. Cancer Lett. 367, 1–11. https://doi.org/10.1016/j.canlet.2015.06.019

Chen, J., Zhang, B., Wong, N., Lo, A.W.I., To, K.-F., Chan, A.W.H., Ng, M.H.L., Ho, C.Y.S., Cheng, S.-H., Lai, P.B.S., Yu, J., Ng, H.-K., Ling, M.-T., Huang, A.-L., Cai, X.-F., Ko, B.C.B., 2011. Sirtuin 1 is upregulated in a subset of hepatocellular carcinomas where it is essential for telomere maintenance and tumor cell growth. Cancer Res. 71, 4138–49. https://doi.org/10.1158/0008-5472.CAN-10-4274

Chen, K.F., Chen, H.L., Tai, W.T., Feng, W.C., Hsu, C.H., Chen, P.J., Cheng, A.L., 2011. Activation of phosphatidylinositol 3-kinase/Akt signaling pathway mediates acquired resistance to sorafenib in hepatocellular carcinoma cells. J. Pharmacol. Exp. Ther. 337, 155–161. https://doi.org/10.1124/jpet.110.175786

Choi, H.-K., Cho, K. Bin, Phuong, N.T.T., Han, C.Y., Han, H.-K., Hien, T.T., Choi, H.S., Kang, K.W., 2013. SIRT1-Mediated FoxO1 Deacetylation Is Essential for Multidrug Resistance-Associated Protein 2 Expression in Tamoxifen-Resistant Breast Cancer Cells. Mol. Pharm. 10, 2517–2527. https://doi.org/10.1021/mp400287p

Chow, A.K.M., Ng, L., Lam, C.S.C., Wong, S.K.M., Wan, T.M.H., Cheng, N.S.M., Yau, T.C.C., Poon, R.T.P., Pang, R.W.C., 2013. The enhanced metastatic potential of hepatocellular carcinoma (HCC) cells with sorafenib resistance. PLoS One 8, e78675.

Cui, J., Guo, Y.-H., Zhang, H.-Y., Jiang, L.-L., Ma, J.-Q., Wang, W.-J., Wang, M.-C., Yang, C.-C., Nan, K.-J., Song, L.-P., 2014. Cyclooxygenase-2 inhibitor is a robust enhancer of anticancer agents against hepatocellular carcinoma multicellular spheroids. Onco. Targets. Ther. 7, 353–63. https://doi.org/10.2147/OTT.S56115

Faivre, S., Rimassa, L., Finn, R.S., 2020. Molecular therapies for HCC: Looking outside the box. J. Hepatol. https://doi.org/10.1016/j.jhep.2019.09.010

Ferretti, A.C., Hidalgo, F., Tonucci, F.M., Almada, E., Pariani, A., Larocca, M.C., Favre, C., 2019. Metformin and glucose starvation decrease the migratory ability of hepatocellular carcinoma cells: targeting AMPK activation to control migration. Sci. Rep. 9, 2815. https://doi.org/10.1038/s41598-019-39556-w

Friedrich, J., Eder, W., Castaneda, J., Doss, M., Huber, E., Ebner, R., Kunz-Schughart, L.A., 2007. A reliable tool to determine cell viability in complex 3-d culture: the acid phosphatase assay. J. Biomol. Screen. 12, 925–37. https://doi.org/10.1177/1087057107306839

Friedrich, J., Seidel, C., Ebner, R., Kunz-Schughart, L.A., 2009. Spheroid-based drug screen: considerations and practical approach. Nat. Protoc. 4, 309–24. https://doi.org/10.1038/nprot.2008.226

Gadaleta-Caldarola, G., Infusino, S., Divella, R., Ferraro, E., Mazzocca, A., De Rose, F., Filippelli, G., Abbate, I., Brandi, M., 2015. Sorafenib: 10 years after the first pivotal trial. Future Oncol. 11, 1863–80. https://doi.org/10.2217/fon.15.85

Garten, A., Grohmann, T., Kluckova, K., Lavery, G.G., Kiess, W., Penke, M., 2019. Sorafenib-induced apoptosis in hepatocellular carcinoma is reversed by SIRT1. Int. J. Mol. Sci. 20. https://doi.org/10.3390/ijms20164048

Gertz, M., Fischer, F., Nguyen, G.T.T., Lakshminarasimhan, M., Schutkowski, M., Weyand, M., Steegborn, C., 2013. Ex-527 inhibits Sirtuins by exploiting their unique NAD+-dependent deacetylation mechanism. Proc. Natl. Acad. Sci. U. S. A. 110, E2772–E2781. https://doi.org/10.1073/pnas.1303628110

Gnoth, M.J., Sandmann, S., Engel, K., Radtke, M., 2010. In vitro to in vivo comparison of the substrate characteristics of sorafenib tosylate toward P-glycoprotein. Drug Metab. Dispos. 38, 1341–6. https://doi.org/10.1124/dmd.110.032052

Hao, C., Zhu, P.-X., Yang, X., Han, Z.-P., Jiang, J.-H., Zong, C., Zhang, X.-G., Liu, W.-T., Zhao, Q.-D., Fan, T.-T., Zhang, L., Wei, L.-X., 2014. Overexpression of SIRT1 promotes metastasis through epithelial-mesenchymal transition in hepatocellular carcinoma. BMC Cancer 14, 978. https://doi.org/10.1186/1471-2407-14-978

Heltweg, B., Gatbonton, T., Schuler, A.D., Posakony, J., Li, H., Goehle, S., Kollipara, R., Depinho, R.A., Gu, Y., Simon, J.A., Bedalov, A., 2006. Antitumor activity of a small-molecule inhibitor of human silent information regulator 2 enzymes. Cancer Res. 66, 4368–77. https://doi.org/10.1158/0008-5472.CAN-05-3617

Hirschhaeuser, F., Menne, H., Dittfeld, C., West, J., Mueller-Klieser, W., Kunz-Schughart, L.A., 2010. Multicellular tumor spheroids: An underestimated tool is catching up again. J. Biotechnol. 148, 3–15.

https://doi.org/10.1016/j.jbiotec.2010.01.012

Holloway, K.R., Calhoun, T.N., Saxena, M., Metoyer, C.F., Kandler, E.F., Rivera, C.A., Pruitt, K., 2010. SIRT1 regulates Dishevelled proteins and promotes transient and constitutive Wnt signaling. Proc. Natl. Acad. Sci. U. S. A. 107, 9216–9221. https://doi.org/10.1073/pnas.0911325107

Hsieh, J.-L., Wu, C.-L., Lee, C.-H., Shiau, A.-L., 2003. Hepatitis B virus X protein sensitizes hepatocellular carcinoma cells to cytolysis induced by E1B-deleted adenovirus through the disruption of p53 function. Clin. Cancer Res. 9, 338–45.

Huang, W.-C., Hsieh, Y.-L., Hung, C.-M., Chien, P.-H., Chien, Y.-F., Chen, L.-C., Tu, C.-Y., Chen, C.-H., Hsu, S.-C., Lin, Y.-M., Chen, Y.-J., 2013. BCRP/ABCG2 inhibition sensitizes hepatocellular carcinoma cells to sorafenib. PLoS One 8, e83627. https://doi.org/10.1371/journal.pone.0083627

Jang, K.Y., Noh, S.J., Lehwald, N., Tao, G.-Z., Bellovin, D.I., Park, H.S., Moon, W.S., Felsher, D.W., Sylvester, K.G., 2012. SIRT1 and c-Myc Promote Liver Tumor Cell Survival and Predict Poor Survival of Human Hepatocellular Carcinomas. PLoS One 7, e45119. https://doi.org/10.1371/journal.pone.0045119

Jiang, X., Feng, K., Zhang, Y., Li, Z., Zhou, F., Dou, H., Wang, T., 2015. Sorafenib and DE605, a novel c-Met inhibitor, synergistically suppress hepatocellular carcinoma. Oncotarget 6, 12340–12356. https://doi.org/10.18632/oncotarget.3656

Jin, Y., Ren, Y., Wu, M., Chen, P., Lu, J., 2015. Effect of shikonin on multidrug resistance in HepG2 : The role of SIRT1. Pharm Biol, Early Online 1–6. https://doi.org/10.3109/13880209.2014.952836

Jung, H.-R., Kang, H.M., Ryu, J.-W., Kim, D.-S., Noh, K.H., Kim, E.-S., Lee, H.-J., Chung, K.-S., Cho, H.-S., Kim, N.-S., Im, D.-S., Lim, J.H., Jung, C.-R., 2017. Cell Spheroids with Enhanced Aggressiveness to Mimic Human Liver Cancer In Vitro and In Vivo. Sci. Rep. 7, 10499. https://doi.org/10.1038/s41598-017-10828-7

Kang, X., Yang, W., Wang, R., Xie, T., Li, H., Feng, D., Jin, X., Sun, H., Wu, S., 2018. Sirtuin-1 (SIRT1) stimulates growth-plate chondrogenesis by attenuating the PERK– eIF-2–CHOP pathway in the unfolded protein response. J. Biol. Chem. 293, 8614–8625. https://doi.org/10.1074/jbc.M117.809822

Kartal-Yandim, M., Adan-Gokbulut, A., Baran, Y., 2016. Molecular mechanisms of drug resistance and its reversal in cancer. Crit. Rev. Biotechnol. 36, 716–726. https://doi.org/10.3109/07388551.2015.1015957

Khawar, I.A., Park, J.K., Jung, E.S., Lee, M.A., Chang, S., Kuh, H.J., 2018. Three Dimensional Mixed-Cell Spheroids Mimic Stroma-Mediated Chemoresistance and Invasive Migration in hepatocellular carcinoma. Neoplasia (United States) 20, 800–812. https://doi.org/10.1016/j.neo.2018.05.008

Kim, H.-B., Lee, S.-H., Um, J.-H., Oh, W.K., Kim, D.-W., Kang, C.-D., Kim, S.-H., 2015. Sensitization of multidrug-resistant human cancer cells to Hsp90 inhibitors by down-regulation of SIRT1. Oncotarget 6, 36202–18. https://doi.org/10.18632/oncotarget.5343

Kim, H.B., Lee, S.H., Um, J.H., Kim, M.J., Hyun, S.K., Gong, E.J., Oh, W.K., Kang, C.D., Kim, S.H., 2015. Sensitization of chemo-resistant human chronic myeloid leukemia stem-like cells to Hsp90 inhibitor by SIRT1 inhibition. Int. J. Biol. Sci. 11, 923–934. https://doi.org/10.7150/ijbs.10896

Lagas, J.S., Van Waterschoot, R.A.B., Sparidans, R.W., Els Wagenaar, J., Beijnen, J.H., Schinkel, A.H., 2010. Breast cancer resistance protein and P-glycoprotein limit sorafenib brain accumulation. Mol. Cancer Ther. 9, 319–326. https://doi.org/10.1158/1535-7163.MCT-09-0663

Langhans, S.A., 2018. Three-dimensional in vitro cell culture models in drug discovery and drug repositioning. Front. Pharmacol. https://doi.org/10.3389/fphar.2018.00006

Laurent, J., Frongia, C., Cazales, M., Mondesert, O., Ducommun, B., Lobjois, V., 2013. Multicellular tumor spheroid models to explore cell cycle checkpoints in 3D. BMC Cancer 13. https://doi.org/10.1186/1471-2407-13-73

Li, Y., Xu, S., Li, J., Zheng, L., Feng, M., Wang, X., Han, K., Pi, H., Li, M., Huang, X., You, N., Tian, Y., Zuo, G., Li, H., Zhao, H., Deng, P., Yu, Z., Zhou, Z., Liang, P., 2016. SIRT1 facilitates hepatocellular carcinoma metastasis by promoting PGC-1α-mediated mitochondrial biogenesis. Oncotarget 7, 29255–74. https://doi.org/10.18632/oncotarget.8711

Liang, X.-J., Finkel, T., Shen, D.-W., Yin, J.-J., Aszalos, A., Gottesman, M.M., 2008. SIRT1 contributes in part to cisplatin resistance in cancer cells by altering mitochondrial metabolism. Mol. Cancer Res. 6, 1499–506. https://doi.org/10.1158/1541-7786.MCR-07-2130

Lin, C.H., Elkholy, K.H., Wani, N.A., Li, D., Hu, P., Barajas, J.M., Yu, L., Zhang, X., Jacob, S.T., Khan, W.N., Bai, X.F., Noonan, A.M., Ghoshal, K., 2020. Ibrutinib Potentiates Antihepatocarcinogenic Efficacy of Sorafenib by Targeting EGFR in Tumor Cells and BTK in Immune Cells in the Stroma. Mol. Cancer Ther. 19, 384–396. https://doi.org/10.1158/1535-7163.MCT-19-0135

Liu, L., Cao, Y., Chen, C., Zhang, X., McNabola, A., Wilkie, D., Wilhelm, S., Lynch, M., Carter, C., 2006. Sorafenib Blocks the RAF/MEK/ERK Pathway, Inhibits Tumor Angiogenesis, and Induces Tumor Cell Apoptosis in Hepatocellular Carcinoma Model PLC/PRF/5. Cancer Res. 66, 11851–11858. https://doi.org/10.1158/0008-5472.CAN-06-1377

Lugrin, J., Ciarlo, E., Santos, A., Grandmaison, G., dos Santos, I., Le Roy, D., Roger, T., 2013. The sirtuin

inhibitor cambinol impairs MAPK signaling, inhibits inflammatory and innate immune responses and protects from septic shock. Biochim. Biophys. Acta 1833, 1498–510. https://doi.org/10.1016/j.bbamcr.2013.03.004

Marshall, G.M., Liu, P.Y., Gherardi, S., Scarlett, C.J., Bedalov, A., Xu, N., Iraci, N., Valli, E., Ling, D., Thomas, W., van Bekkum, M., Sekyere, E., Jankowski, K., Trahair, T., MacKenzie, K.L., Haber, M., Norris, M.D., Biankin, A. V., Perini, G., Liu, T., 2011. SIRT1 Promotes N-Myc Oncogenesis through a Positive Feedback Loop Involving the Effects of MKP3 and ERK on N-Myc Protein Stability. PLoS Genet. 7, e1002135. https://doi.org/10.1371/journal.pgen.1002135

Mehta, G., Hsiao, A.Y., Ingram, M., Luker, G.D., Takayama, S., 2012. Opportunities and challenges for use of tumor spheroids as models to test drug delivery and efficacy. J. Control. Release 164, 192–204. https://doi.org/10.1016/j.jconrel.2012.04.045

Mittler, F., Obeïd, P., Rulina, A. V, Haguet, V., Gidrol, X., Balakirev, M.Y., 2017. High-Content Monitoring of Drug Effects in a 3D Spheroid Model. Front. Oncol. 7, 293. https://doi.org/10.3389/fonc.2017.00293

Napper, A.D., Hixon, J., McDonagh, T., Keavey, K., Pons, J.F., Barker, J., Yau, W.T., Amouzegh, P., Flegg, A., Hamelin, E., Thomas, R.J., Kates, M., Jones, S., Navia, M.A., Saunders, J.O., DiStefano, P.S., Curtis, R., 2005. Discovery of indoles as potent and selective inhibitors of the deacetylase SIRT1. J. Med. Chem. 48, 8045–8054. https://doi.org/10.1021/jm050522v

Niu, L., Liu, L., Yang, S., Ren, J., Lai, P.B.S., Chen, G.G., 2017. New insights into sorafenib resistance in hepatocellular carcinoma: Responsible mechanisms and promising strategies. Biochim. Biophys. Acta - Rev. Cancer. https://doi.org/10.1016/j.bbcan.2017.10.002

Peck, B., Chen, C.Y., Ho, K.K., Di Fruscia, P., Myatt, S.S., Coombes, R.C., Fuchter, M.J., Hsiao, C.D., Lam, E.W.F., 2010. SIRT Inhibitors Induce Cell Death and p53 Acetylation through Targeting Both SIRT1 and SIRT2. Mol. Cancer Ther. 9, 844–855.

Ponnusamy, M., Zhou, X., Yan, Y., Tang, J., Tolbert, E., Zhao, T.C., Gong, R., Zhuang, S., 2014. Blocking sirtuin 1 and 2 inhibits renal interstitial fibroblast activation and attenuates renal interstitial fibrosis in obstructive nephropathy. J. Pharmacol. Exp. Ther. 350, 243–256. https://doi.org/10.1124/jpet.113.212076

Portmann, S., Fahrner, R., Lechleiter, A., Keogh, A., Overney, S., Laemmle, A., Mikami, K., Montani, M., Tschan, M.P., Candinas, D., Stroka, D., 2013. Antitumor effect of SIRT1 inhibition in human HCC tumor models in vitro and in vivo. Mol. Cancer Ther. 12, 499–508. https://doi.org/10.1158/1535-7163.MCT-12-0700

Pruitt, K., Zinn, R.L., Ohm, J.E., McGarvey, K.M., Kang, S.-H.L., Watkins, D.N., Herman, J.G., Baylin, S.B., 2006. Inhibition of SIRT1 Reactivates Silenced Cancer Genes without Loss of Promoter DNA Hypermethylation. PLoS Genet. 2, e40. https://doi.org/10.1371/journal.pgen.0020040

Sedmak, J.J., Grossberg, S.E., 1977. A Rapid, Sensitive and Versatile Assay for Protein Using Coomassie Brilliant Blue G250. Anal. Biochem. 79, 544–552.

Singh, S., Kumar, P.U., Thakur, S., Kiran, S., Sen, B., Sharma, S., Rao, V.V., Poongothai, A.R., Ramakrishna, G., 2015. Expression/localization patterns of sirtuins (SIRT1, SIRT2, and SIRT7) during progression of cervical cancer and effects of sirtuin inhibitors on growth of cervical cancer cells. Tumor Biol. 36, 6159–6171. https://doi.org/10.1007/s13277-015-3300-y

Sun, C.K., Chua, M.S., He, J., So, S.K., 2011. Suppression of glypican 3 inhibits growth of hepatocellular carcinoma cells through up-regulation of TGF-β2. Neoplasia 13, 735–747. https://doi.org/10.1593/neo.11664

Süssmuth, S.D., Haider, S., Landwehrmeyer, G.B., Farmer, R., Frost, C., Tripepi, G., Andersen, C.A., Di Bacco, M., Lamanna, C., Diodato, E., Massai, L., Diamanti, D., Mori, E., Magnoni, L., Dreyhaupt, J., Schiefele, K., Craufurd, D., Saft, C., Rudzinska, M., Ryglewicz, D., Orth, M., Brzozy, S., Baran, A., Pollio, G., Andre, R., Tabrizi, S.J., Darpo, B., Westerberg, G., 2015. An exploratory double-blind, randomized clinical trial with selisistat, a SirT1 inhibitor, in patients with Huntington's disease. Br. J. Clin. Pharmacol. 79, 465–476. https://doi.org/10.1111/bcp.12512

Tomonari, T., Takeishi, S., Taniguchi, T., Tanaka, T., 2016. MRP3 as a novel resistance factor for sorafenib in hepatocellular carcinoma. Oncotarget 7, 1–9. https://doi.org/10.18632/oncotarget.6889

Tsou, S.-H., Hou, M.-H., Hsu, L.-C., Chen, T.-M., Chen, Y.-H., 2015. Gain-of-function p53 mutant with 21-bp deletion confers susceptibility to multidrug resistance in MCF-7 cells. Int. J. Mol. Med. 37, 233–42. https://doi.org/10.3892/ijmm.2015.2406

Vinci, M., Gowan, S., Boxall, F., Patterson, L., Zimmermann, M., Court, W., Lomas, C., Mendiola, M., Hardisson, D., Eccles, S.A., 2012. Advances in establishment and analysis of three-dimensional tumor spheroid-based functional assays for target validation and drug evaluation. BMC Biol. 10, 29. https://doi.org/10.1186/1741-7007-10-29

Wang, J., Zhu, X.X., Liu, L., Xue, Y., Yang, X., Zou, H.J., 2016. SIRT1 prevents hyperuricemia via the PGC-1α/PPARγ-ABCG2 pathway. Endocrine 53, 443–452. https://doi.org/10.1007/s12020-016-0896-7

Wang, M., Wang, Z., Zhi, X., Ding, W., Xiong, J., Tao, T., Yang, Y., Zhang, H., Zi, X., Zhou, W., Huang, G.,

2020. SOX9 enhances sorafenib resistance through upregulating ABCG2 expression in hepatocellular carcinoma. Biomed. Pharmacother. 129, 110315. https://doi.org/10.1016/j.biopha.2020.110315

Wang, Y., He, J., Liao, M., Hu, M., Li, W., Ouyang, H., Wang, X., Ye, T., Zhang, Y., Ouyang, L., 2019. An overview of Sirtuins as potential therapeutic target: Structure, function and modulators. Eur. J. Med. Chem. https://doi.org/10.1016/j.ejmech.2018.10.028

Wen, X., Ling, S., Wu, W., Shan, Q., Liu, P., Wang, C., Wei, X., Ding, W., Teng, X., Xu, X., 2020. Ubiquitin-Specific Protease 22/Silent Information Regulator 1 Axis Plays a Pivotal Role in the Prognosis and 5-Fluorouracil Resistance in Hepatocellular Carcinoma. Dig. Dis. Sci. 65, 1064. https://doi.org/10.1007/s10620-019-05844-8

Westerberg, G., Chiesa, J.A., Andersen, C.A., Diamanti, D., Magnoni, L., Pollio, G., Darpo, B., Zhou, M., 2015. Safety, pharmacokinetics, pharmacogenomics and QT concentration-effect modelling of the SirT1 inhibitor selisistat in healthy volunteers. Br. J. Clin. Pharmacol. 79, 477–491. https://doi.org/10.1111/bcp.12513

Wu, G., Song, C., Lu, H., Jia, L., Yang, G., Shi, X., Sun, S., 2014. Sirt2 Induces C2C12 Myoblasts Proliferation by Activation of the ERK1/2 Pathway. Acta Biochim. Biophys. Sin. (Shanghai). 46. https://doi.org/10.1093/ABBS/GMT151

Wu, Y., Meng, X., Huang, C., Li, J., 2015. Emerging role of silent information regulator 1 (SIRT1) in hepatocellular carcinoma: a potential therapeutic target. Tumor Biol. https://doi.org/10.1007/s13277-015-3488-x

Xie, H.J., Jung, K.H., Nam, S.W., 2011. Overexpression of SIRT2 contributes tumor cell growth in hepatocellular carcinomas. Mol. Cell. Toxicol. 7, 367–374. https://doi.org/10.1007/s13273-011-0046-5

Xu, W.-H., Han, M., Dong, Q., Fu, Z.-X., Diao, Y.-Y., Liu, H., Xu, J., Jiang, H.-L., Zhang, S.-Z., Zheng, S., Gao, J.-Q., Wei, Q.-C., 2012. Doxorubicin-mediated radiosensitivity in multicellular spheroids from a lung cancer cell line is enhanced by composite micelle encapsulation. Int. J. Nanomedicine 7, 2661–71. https://doi.org/10.2147/IJN.S30445

Zastawny, R.L., Salvino, R., Chen, J., Benchimol, S., Ling, V., 1993. The core promoter region of the P-glycoprotein gene is sufficient to confer differential responsiveness to wild-type and mutant p53. Oncogene 8, 1529–35.

Zhu, H., Xia, L., Zhang, Y., Wang, H., Xu, W., Hu, H., Wang, J., Xin, J., Gang, Y., Sha, S., Xu, B., Fan, D., Nie, Y., Wu, K., 2012. Activating transcription factor 4 confers a multidrug resistance phenotype to gastric

cancer cells through transactivation of SIRT1 expression. PLoS One 7, e31431. https://doi.org/10.1371/journal.pone.0031431

Fig. 1. Effect of SIRTs inhibitors on cellular viability and colony formation upon sorafenib treatment conditions in 2D cultures. A) MTT assay: HCC cells were incubated for 72 h with different doses of sorafenib to obtain the dose-response curves. **B)** MTT assay: HepG2 and Huh7 cells were incubated for 72 h with 2 μM or 1 μM sorafenib (Sfb 2 or Sfb 1), respectively, alone or in combination with 50 μM cambinol (Sfb + Camb 50) or 40 μM EX-527 (Sfb + EX 40). Also, HCC cells were treated with 50 μM cambinol (Camb 50) or 40 μM EX-527 (EX 40) in the absence of sorafenib. **A, B)** Cell viability is expressed in percent value with control cells arbitrarily considered 100%. At least 3 independent experiments; n=3 in each one. **C)** Clonogenic assay: HepG2 and Huh7 cells were treated as in **B)** and then were grown in fresh culture media for 7 days. Representative wells are shown for both HCC cell lines. Data are expressed as a percentage of colonies in control cells (arbitrarily considered 100%) of three independent experiments, each of which was performed in duplicate. Mean ± S.E.M; *$P < 0.05$ vs. control; $^{\#}P < 0.05$ vs. Sfb; $^{\$}P < 0.05$ vs. Camb 50; $^{\&}P < 0.05$ vs. EX 40.

Fig. 2. Effect of cambinol and EX-527 on spheroid viability during sorafenib treatment. APH assay: **A)** 3D cultures of HCC cells were incubated for 72 h with different doses of sorafenib to obtain the dose-response curves. **B)** 3D cultures of HepG2 and Huh7 cells were incubated for 72 h with 4 μM or 2 μM sorafenib (Sfb 4 or Sfb 2), respectively, alone or in combination with 50 μM cambinol (Sfb + Camb 50) or 80 μM or 40 μM EX-527 (Sfb + EX 80 or Sfb + EX 40), respectively. Also, 3D cultures were treated with 50 μM cambinol (Camb 50) or 80 μM EX-527 (EX 80) for HepG2 and 40 μM EX-527 (EX 40) for Huh7 in the absence of sorafenib. **A, B)** Cell viability is expressed in percent value with control spheroids arbitrarily considered 100%. At least 3 independent experiments; n=8 in each one. Mean ± S.E.M; *$P < 0.05$ vs. control; $^{\#}P < 0.05$ vs. Sfb; $^{\$}P < 0.05$ vs. Camb 50; $^{\&}P < 0.05$ vs. EX.

Fig. 3. Effect of SIRTs inhibitors on proliferation upon sorafenib treatment conditions in 2D cultures. HepG2 and Huh7 cells were incubated for 72 h with 2 μM or 1 μM sorafenib (Sfb 2 or Sfb 1), respectively, alone or in combination with 50 μM cambinol (Sfb + Camb 50) or 40 μM EX-527 (Sfb + EX 40). Also, HCC cells were treated with 50 μM cambinol (Camb 50) or 40 μM EX-527 (EX 40) in the absence of sorafenib. **A, B)** Western blot: **A)** PCNA and **B)** cyclin D1 protein levels. β-actin was probed as loading control. Selected lanes

were cropped from different parts of the same gel and they are shown after cropping, aligning and separating them by a white space. Densitometric analysis was performed and results are expressed in percent values with control cells arbitrarily considered 100%. Three independent experiments; n = 3 in each one. **C)** Cell cycle analysis: Cells were fixed, stained with propidium iodide, and their distribution in cell cycle was analyzed by flow cytometry. Bar charts show the percentage of cells in G0/G1 and S phases of the cell cycle. Two independent experiments; n = 3 in each one. Mean ± S.E.M; *P < 0.05 vs. control; $^{\#}$P < 0.05 vs. Sfb; $^{\$}$P < 0.05 vs. Camb 50; $^{\&}$P < 0.05 vs. EX 40.

Fig. 4. Effect of cambinol and EX-527 on spheroid growth during sorafenib treatment. Spheroid growth delay assay: **A)** 3D cultures of HCC cells were incubated for 72 h with different doses of sorafenib to obtain the dose-response curves. **B, C)** 3D cultures of HepG2 and Huh7 cells were incubated for 72 h with 4 μM or 2 μM sorafenib (Sfb 4 or Sfb 2), respectively, alone or in combination with 50 μM cambinol (Sfb + Camb 50) or 80 μM or 40 μM EX-527 (Sfb + EX 80 or Sfb + EX 40), respectively. Also, 3D cultures were treated with 50 μM cambinol (Camb 50) or 80 μM EX-527 (EX 80) for HepG2 and 40 μM EX-527 (EX 40) for Huh7 in the absence of sorafenib. **B)** Representative images of spheroids before (0 h) and after 72 h of treatment are shown for both HCC cell lines. Scale bar 200 μm. **A, C)** Results are expressed as the percentage of volume at 72 h vs. 0 h with control spheroids arbitrarily considered 100%. At least 3 independent experiments; n=8 in each one. Mean ± S.E.M; *P < 0.05 vs. control; $^{\#}$P < 0.05 vs. Sfb; $^{\$}$P < 0.05 vs. Camb 50; $^{\&}$P < 0.05 vs. EX.

Fig. 5. Effect of SIRTs inhibitors on spheroid proliferation upon sorafenib treatment conditions. Immunofluorescence: 3D cultures of HepG2 and Huh7 cells were incubated for 72 h with 4 μM or 2 μM sorafenib (Sfb 4 or Sfb 2), respectively, alone or in combination with 50 μM cambinol (Sfb + Camb 50) or 80 μM or 40 μM EX-527 (Sfb + EX 80 or Sfb + EX 40), respectively. Also, 3D cultures were treated with 50 μM cambinol (Camb 50) or 80 μM EX-527 (EX 80) for HepG2 and 40 μM EX-527 (EX 40) for Huh7 in the absence of sorafenib. Representative images of spheroids sections of **A)** HepG2 and **B)** Huh7 cells visualized by confocal microscopy showing the expression of Ki-67 in green and PCNA and cyclin D1 in red. Nuclei were stained with DAPI (blue). Scale bar 200 μm. The fraction of the proliferation marker-positive cells (proliferation marker/DAPI) and the total number of the proliferation marker-positive cells per section of spheroid is shown for **C)** Ki-67, **D)** PCNA and **E)** cyclin D1. Results are expressed in percent value with control spheroids arbitrarily

considered 100%. Two independent experiments; n=8. Mean ± S.E.M; *P < 0.05 vs. control; $^{\#}$P < 0.05 vs. Sfb; $^{\$}$P < 0.05 vs. Camb; $^{\&}$P < 0.05 vs. EX.

Fig. 6. Effect of cambinol and EX-527 on apoptosis upon sorafenib treatment conditions in 2D cultures. HepG2 and Huh7 cells were incubated for 72 h with 2 μM or 1 μM sorafenib (Sfb 2 or Sfb 1), respectively, alone or in combination with 50 μM cambinol (Sfb + Camb 50) or 40 μM EX-527 (Sfb + EX 40). Also, HCC cells were treated with 50 μM cambinol (Camb 50) or 40 μM EX-527 (EX 40) in the absence of sorafenib. **A)** Annexin V/propidium iodide assay: Early (EA) and late (LA) apoptosis is expressed in percent value with control cells arbitrarily considered 100%. Three independent experiments, each of which was performed in duplicate. Mean ± S.E.M; *P < 0.05 vs. control; $^{\#}$P < 0.05 vs. Sfb; $^{\$}$P < 0.05 vs. Camb 50; $^{\&}$P < 0.05 vs. EX 40. **B)** Caspase-3/7 activation assay: Representative images are shown for cells stained with CellEvent™ Caspase-3/7 Green ReadyProbes™ Reagent for 30 min and observed under fluorescent microscope. Green fluorescence corresponds to caspase-3/7-positive cells.

Fig. 7. Effect of SIRTs inhibitors on spheroid apoptosis during sorafenib treatment. Caspase-3/7 activation assay: 3D cultures of HepG2 and Huh7 cells were incubated for 72 h with 4 μM or 2 μM sorafenib (Sfb 4 or Sfb 2), respectively, alone or in combination with 50 μM cambinol (Sfb + Camb 50) or 80 μM or 40 μM EX-527 (Sfb + EX 80 or Sfb + EX 40), respectively. Also, 3D cultures were treated with 50 μM cambinol (Camb 50) or 80 μM EX-527 (EX 80) for HepG2 and 40 μM EX-527 (EX 40) for Huh7 in the absence of sorafenib. **A)** Representative images are shown for spheroids stained with CellEvent™ Caspase-3/7 Green ReadyProbes™ Reagent for 1 h and observed under fluorescent microscope. Green fluorescence corresponds to caspase-3/7 activation. The white dotted line corresponds to the edge of the spheroid. Scale bar 200 μm. **B)** Data are expressed as the percentage of apoptosis in control spheroids (arbitrarily considered 100%). Three independent experiments; n = 2 in each one. Mean ± S.E.M; *P < 0.05 vs. control; $^{\#}$P < 0.05 vs. Sfb; $^{\$}$P < 0.05 vs. Camb 50; $^{\&}$P < 0.05 vs. EX.

Fig. 8. Effect of cambinol and EX-527 on migration and invasion during sorafenib treatment in 2D cultures. A, B) Wound healing assay: HepG2 and Huh7 cells were treated with 2 μM or 1 μM sorafenib (Sfb 2 or Sfb 1), respectively, alone or in combination with 50 μM cambinol (Sfb + Camb 50) or 40 μM EX-527 (Sfb + EX 40). Also, HCC cells were treated with 50 μM cambinol (Camb 50) or 40 μM EX-527 (EX 40) in the

absence of sorafenib. **A)** Representative wound images are shown before and after 24 h of treatment. **B)** The distance migrated by cells is expressed in percent value with control cells arbitrarily considered 100%. **C)** Transwell cell invasion assay: Huh7 cells were treated as above. Representative images of cells that invaded the lower chamber after 48 h of treatment are shown. Cellular invasion is expressed in percent value with control cells arbitrarily considered 100%. **A-C)** Three independent experiments; 18 fields/well and 15 fields/well for wound healing and transwell cell invasion assays, respectively, in each experiment. Mean ± S.E.M; *P < 0.05 vs. control; $^{\#}$P < 0.05 vs. Sfb; $^{\$}$P < 0.05 vs. Camb 50; $^{\&}$P < 0.05 vs. EX 40.

Fig. 9. Effect of SIRTs inhibitors on spheroid migration upon sorafenib treatment conditions. Spheroid migration assay: 3D cultures of Huh7 cells were incubated for 48 h and 72 h with 2 μM sorafenib (Sfb 2), alone or in combination with 50 μM cambinol (Sfb + Camb 50) or 40 μM EX-527 (Sfb + EX 40). Also, 3D cultures of Huh7 cells were treated with 50 μM cambinol (Camb 50) or 40 μM EX-527 (EX 40) in the absence of sorafenib. **A)** Representative images of migrating spheroids before (0 h) and after 48 h and 72 h of treatment. The black dotted line corresponds to the migration front. Scale bar 200 μm. **B)** Data are expressed as the percentage of migrated area in control spheroids (arbitrarily considered 100%). Three independent experiments; n = 8 in each one. Mean ± S.E.M; *P < 0.05 vs. control; $^{\#}$P < 0.05 vs. Sfb 2; $^{\$}$P < 0.05 vs. Camb 50.

Fig. 10. Effect of cambinol and EX-527 on ABC transporters expression during sorafenib treatment in 2D cultures. Western blot: HepG2 and Huh7 cells were incubated for 72 h with 2 μM or 1 μM sorafenib (Sfb 2 or Sfb 1), respectively, alone or in combination with 50 μM cambinol (Sfb + Camb 50) or 40 μM EX-527 (Sfb + EX 40). Also, HCC cells were treated with 50 μM cambinol (Camb 50) or 40 μM EX-527 (EX 40) in the absence of sorafenib. **A)** P-gp, **B)** MRP3, **C)** BCRP and **D)** MRP2 protein levels. β-actin was probed as loading control. Selected lanes were cropped from different parts of the same gel and they are shown after cropping, aligning and separating them by a white space. Densitometric analysis was performed and results are expressed in percent values with control cells arbitrarily considered 100%. Three independent experiments; n = 3 in each one. Mean ± S.E.M; *P < 0.05 vs. control; $^{\#}$P < 0.05 vs. Sfb; $^{\$}$P < 0.05 vs. Camb 50; $^{\&}$P < 0.05 vs. EX 40.

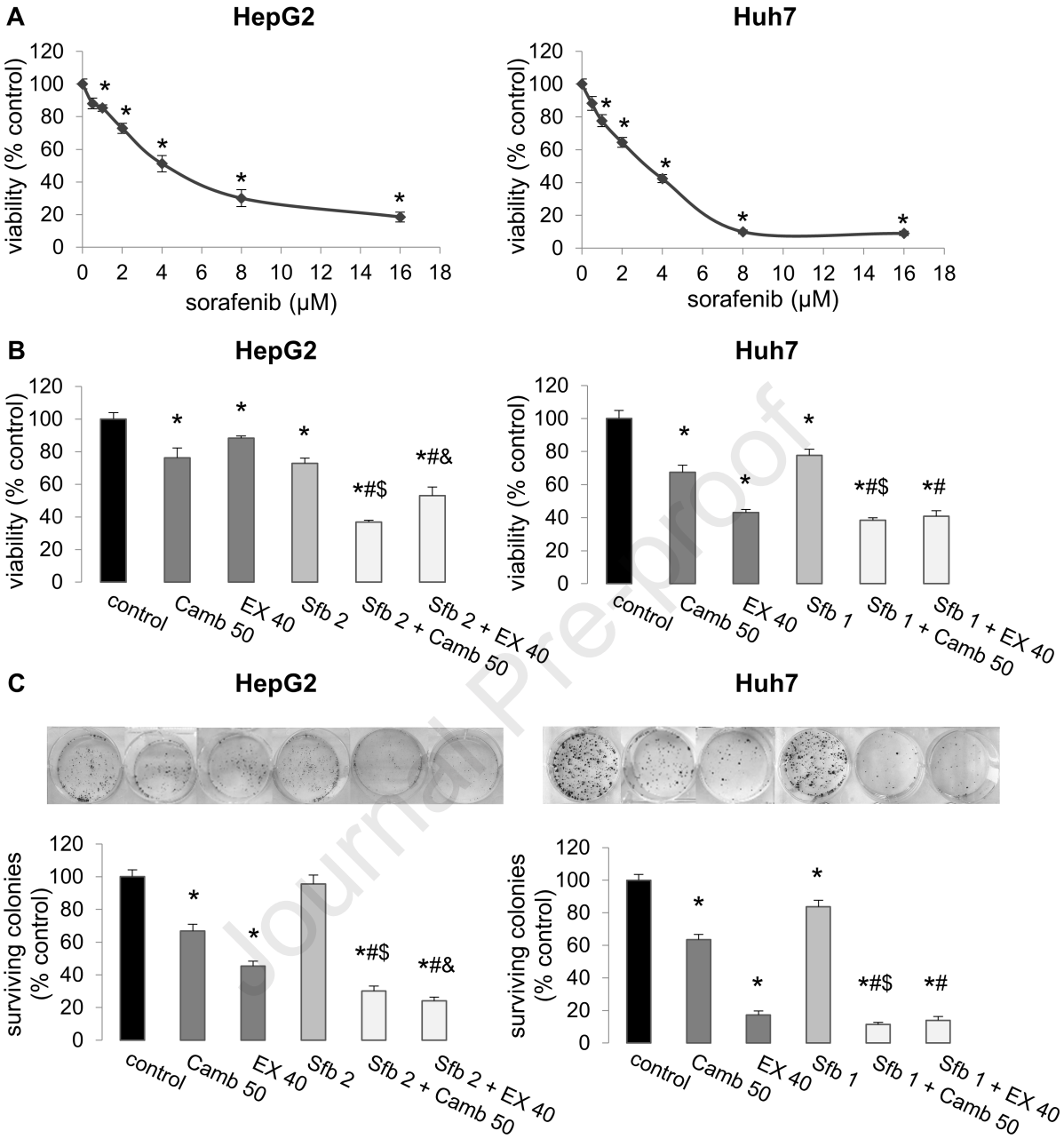

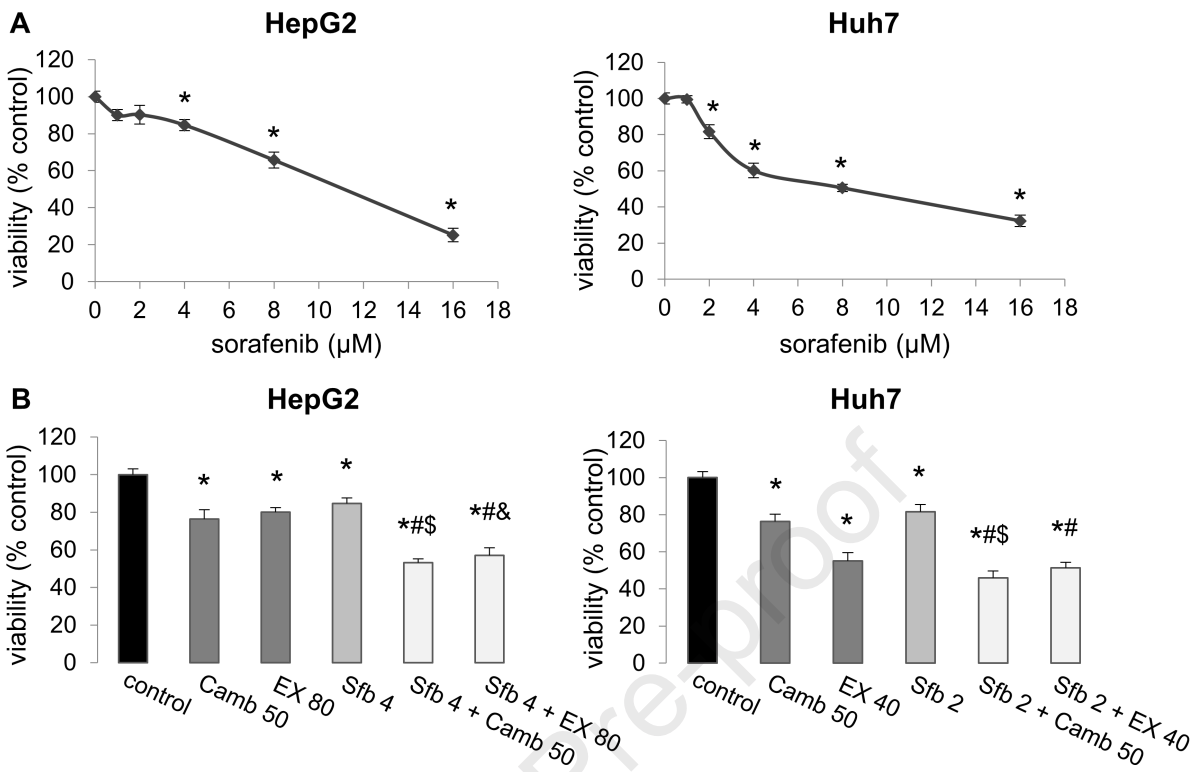

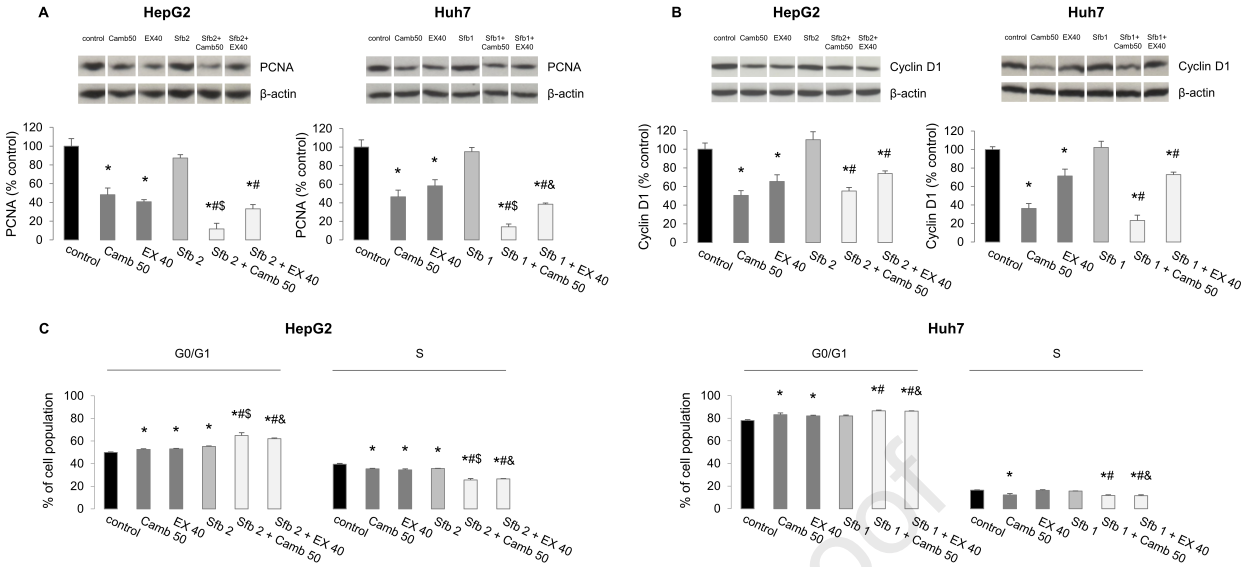

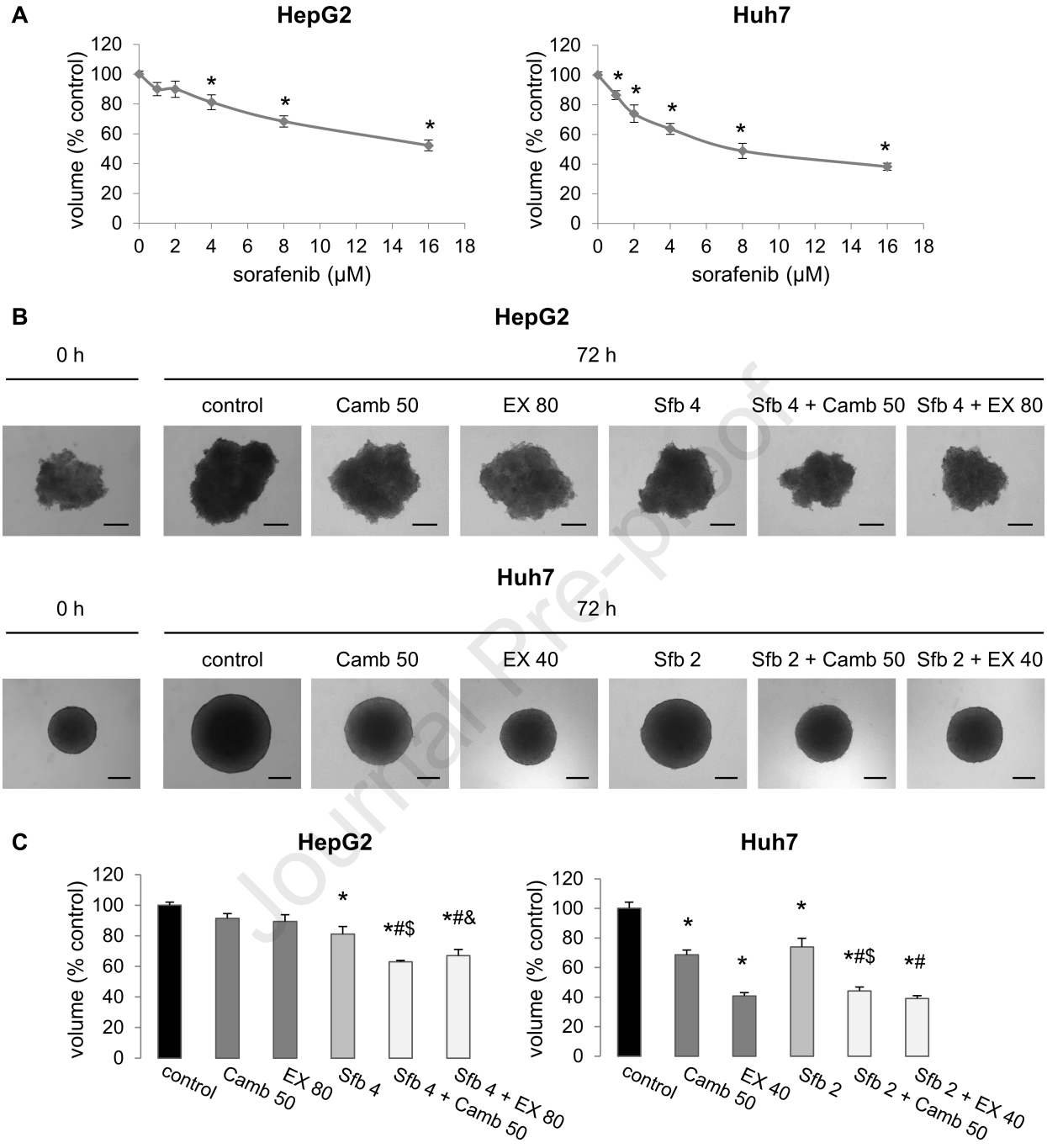

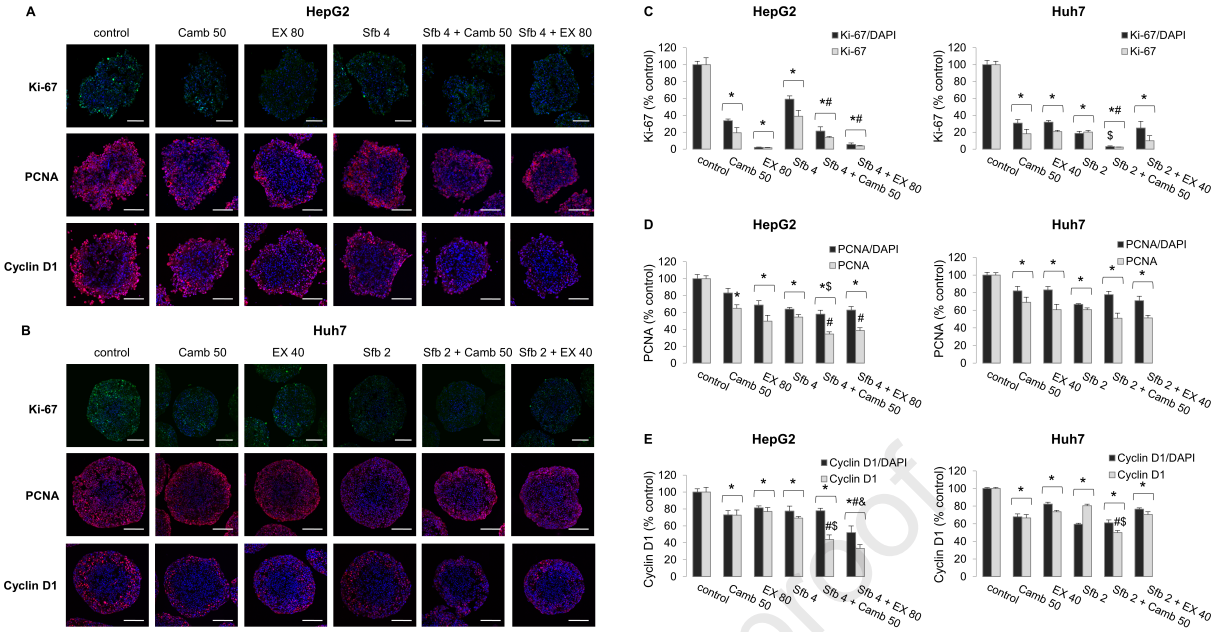

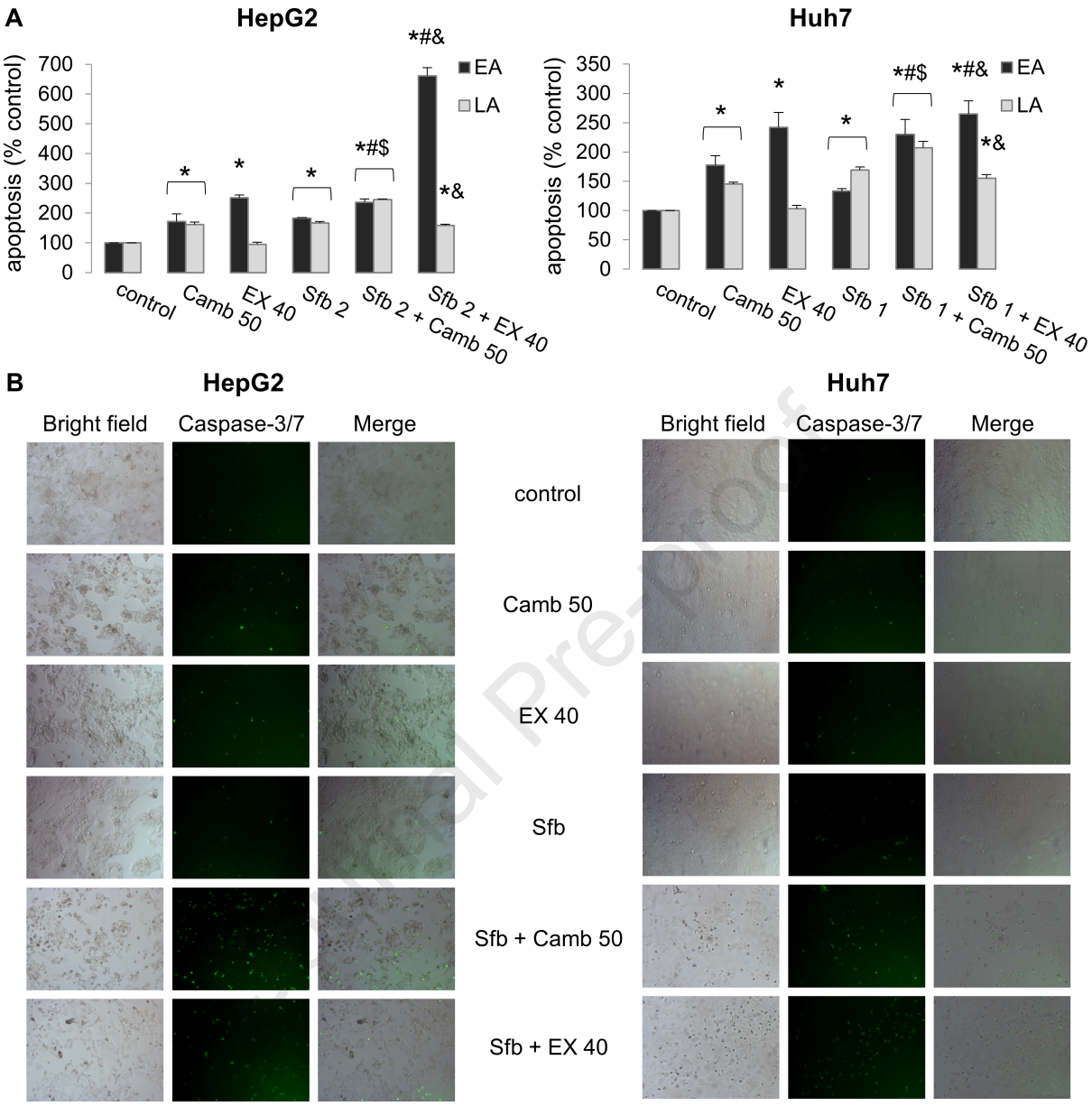
A
HepG2
apoptosis (% control)
700
600
500
400
300
200
100
0
EA
LA
*
*
*
*#$
*#&
*&
control
Camb 50
EX 40
Sfb 2
Sfb 2 + Camb 50
Sfb 2 + EX 40
Huh7
apoptosis (% control)
350
300
250
200
150
100
50
0
*
*
*
*#$
*#&
*&
control
Camb 50
EX 40
Sfb 1
Sfb 1 + Camb 50
Sfb 1 + EX 40
B
HepG2
Bright field
Caspase-3/7
Merge
control
Camb 50
EX 40
Sfb
Sfb + Camb 50
Sfb + EX 40
Huh7
Bright field
Caspase-3/7
Merge

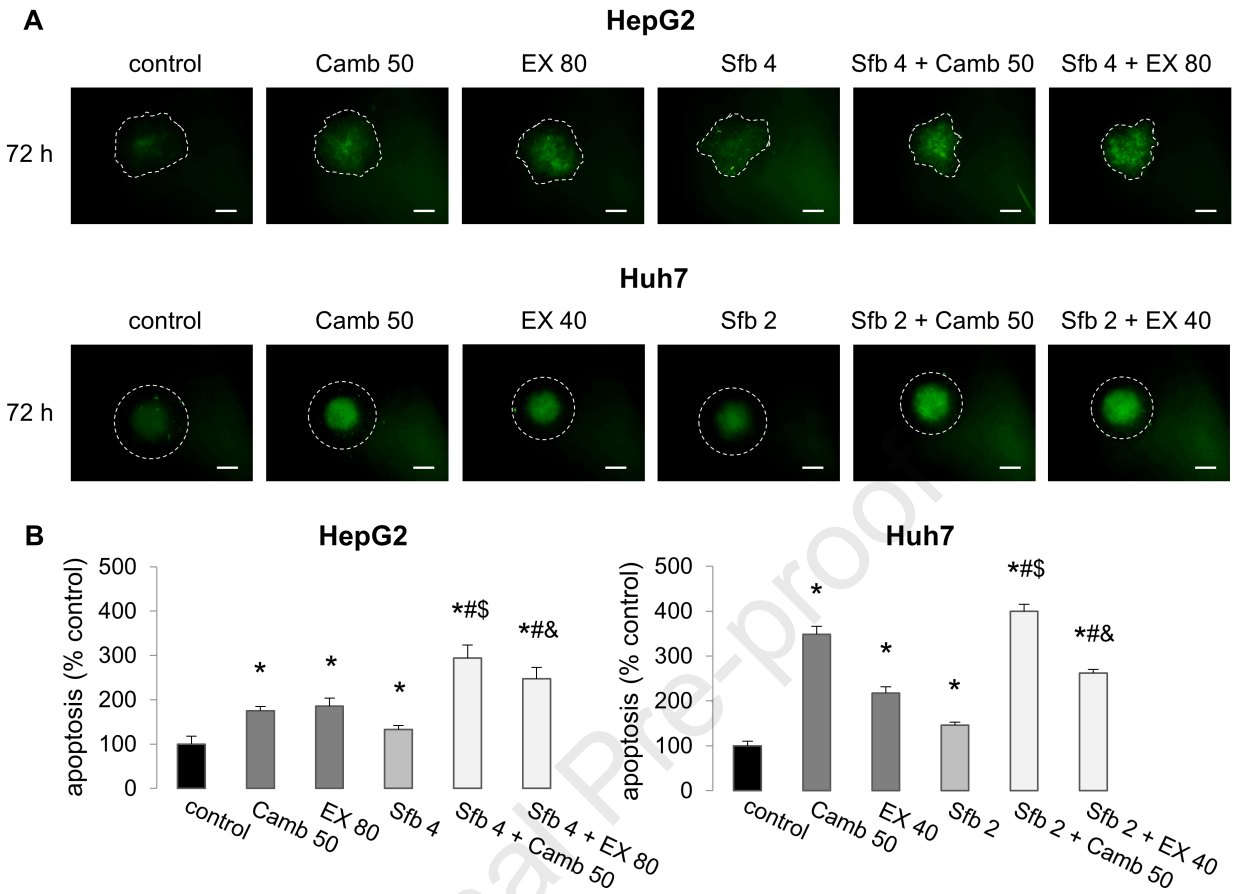

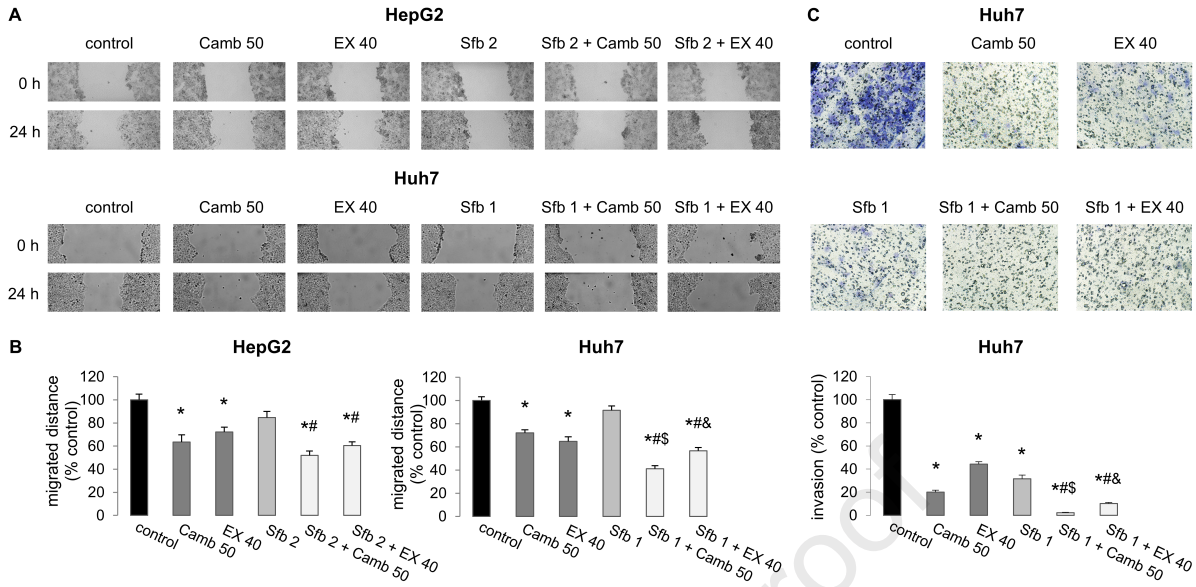

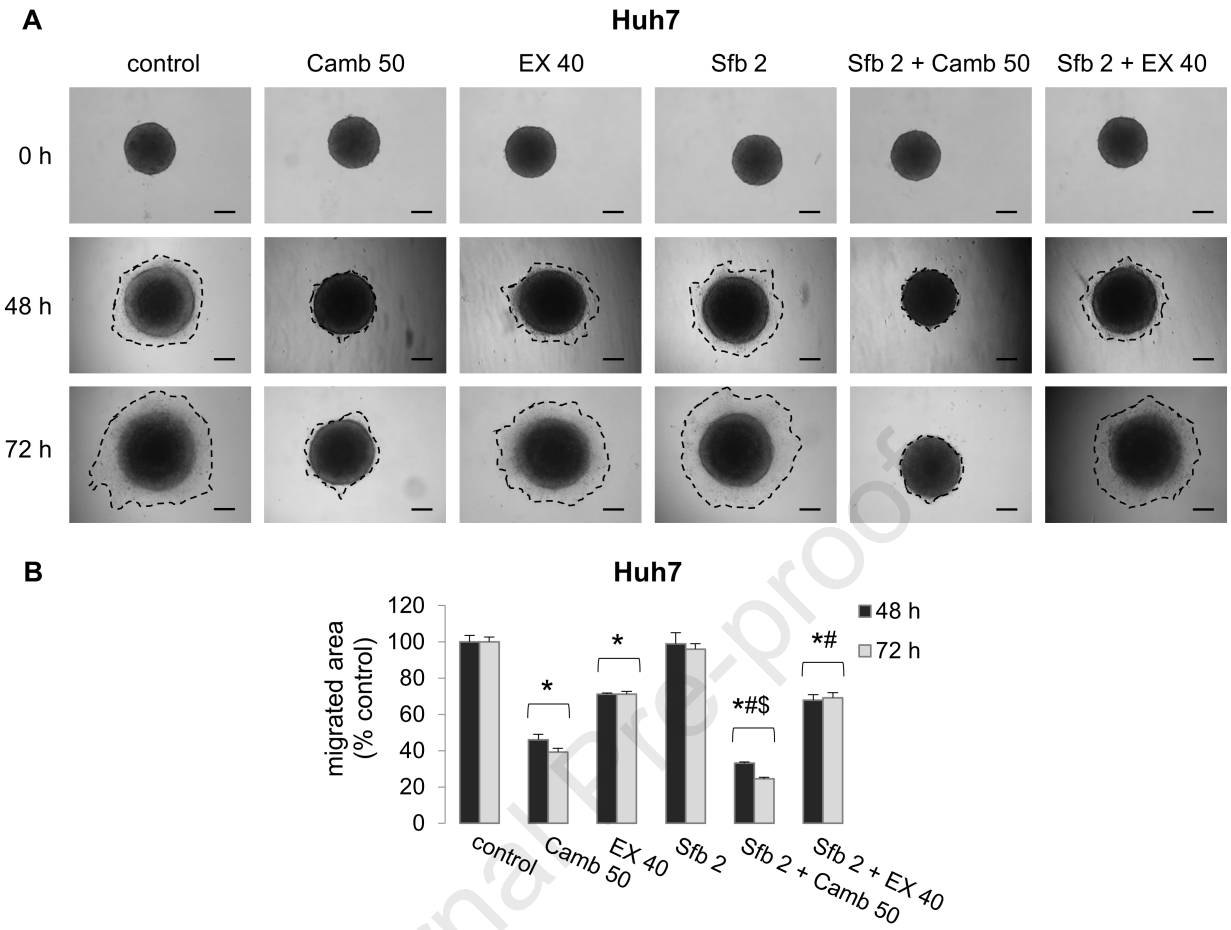

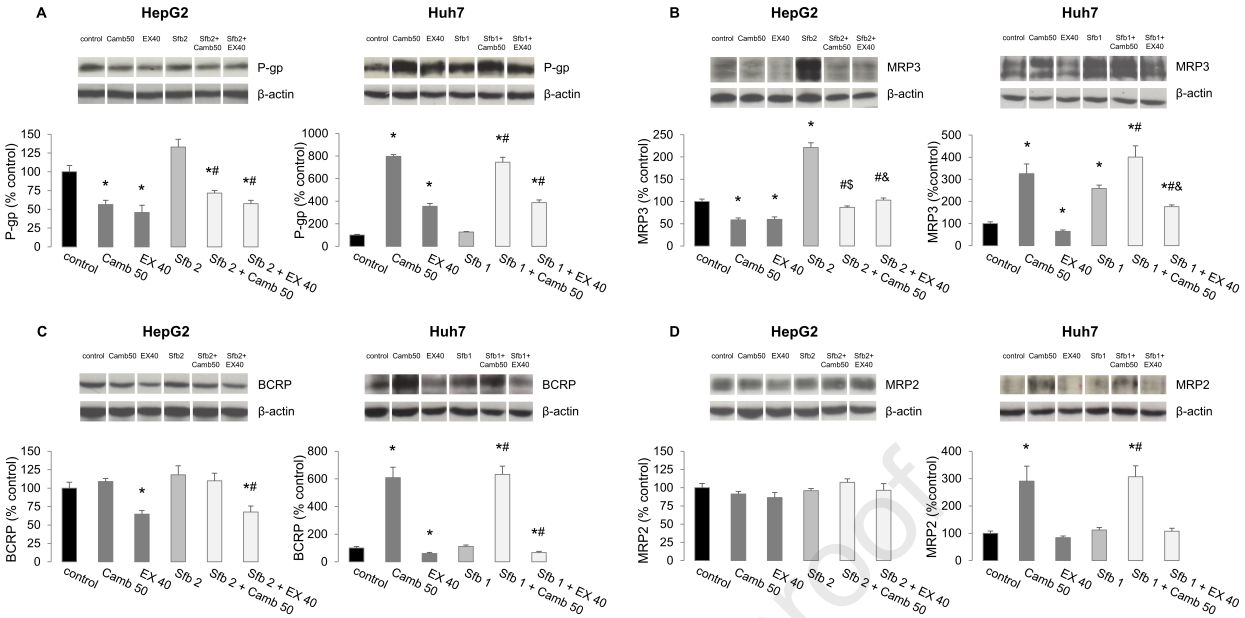

Declaration of interests

☒ The authors declare that they have no known competing financial interests or personal relationships that could have appeared to influence the work reported in this paper.

☐The authors declare the following financial interests/personal relationships which may be considered as potential competing interests: